EXPERIMENTAL HEAT TRANSFER AT HYPERSONIC MACH NUMBER

Thesis by

Richard D. DeLauer

LT. USN

In Partial Fulfillment of the Requirements

For the Degree of

Doctor of Philosophy

California Institute of Technology

Pasadena, California

1953

ACKNOWLEDGMENTS

The writer wishes to thank his advisor, Dr. H. T. Nagamatsu, for his suggestions, encouragement, and whole hearted support throughout this investigation.

The author also wishes to express his sincere gratitude to the Naval Postgraduate School and the Bureau of Aeronautics of the Navy Department, whose interest, support, and policies made his graduate study possible.

Helpful suggestions and criticisms by other staff members, particularly Drs. H. W. Liepmann and J. D. Cole, are gratefully acknowledged.

To Mr. C. A. Bartsch and his co-workers in the GALCIT Machine Shop, whose skill contributed to the successful fabrication of the model, and to the staff of the GALCIT 5 x 5 inch Hypersonic Wind Tunnel for their help during the complete program, the writer is indebted.

A special mention is due to Miss F. Scheinis, Mrs. B. Wood, and Miss J. Mainwaring for their help in making the necessary computations and preparation of the curves for the final thesis copy. In addition, thanks are extended to Mrs. G. Van Gieson who prepared the manuscript and to Mrs. C. Rade and Miss M. Baker who did the reproduction.

The writer finally wishes to thank his wife, Ann, for her patience and tolerance which played an important part in the completion of this investigation.

ABSTRACT

An experimental investigation was conducted in Leg 1 of the GALCIT 5 x 5 inch Hypersonic Wind Tunnel to determine the heat transfer coefficients of the laminar boundary layer on a cooled flat plate at a nominal Mach number of 5.8. As a consequence of the investigation, flat plate recovery factors were determined and the effect of condensation on heat transfer was noted. In addition qualitative results as to the laminar boundary layer transition and separation are also presented.

The tests were conducted with a ratio of wall temperature to free stream temperature (T_w/T_δ) of approximately 6.2; but under stagnation temperature conditions ranging from 200°F to 285°F. The stagnation pressure range of 60 psia to 115.5 psia provided a maximum Reynolds number of 2.1×10^6.

A flat plate temperature recovery factor of $.858 \pm .004$ was determined, and it was concluded that the temperature recovery factor range of Mach number independence could be extended to a Mach number of 5.8. The independence of the recovery factor on Reynolds number up to the beginning of the laminar boundary layer transition was also substantiated.

The heat transfer coefficients were obtained for a negative temperature gradient over a considerable portion of the plate. The effect of these gradients produced values considerably higher than would be expected for an isothermal surface. These results, when related to the constant temperature case by a theoretical calculation, were in good agreement with the theoretical results and the results of a skin friction investigation carried out at the same Mach number. The accuracy

of the results was estimated to be ±10% from a value of $Nu/Re^{1/2} Pr^{1/3}$ = .285.

There was no apparent effect on the heat transfer coefficient by condensation, but the adiabatic wall temperature appeared to be 2% lower than for the condensation free flow. Due to a step increase in thickness of the model at the ten inch station, the shock wave-boundary layer interaction appears to produce laminar boundary layer transition at a Reynolds number of 1.3×10^6, and upon reducing the Reynolds number further, the transition point is subjected to an adverse pressure gradient which results in a boundary layer separation.

TABLE OF CONTENTS

NOMENCLATURE

Symbols

a = speed of sound, ft/sec

A = area sq ft

c_f = local skin friction coefficient, dimensionless

c_p = specific heat at constant pressure Btu/(lb)(deg F)

f_c = convective conductance, Btu/(sq ft)(deg F)

$\bar{F}$ = radiation geometric factor, dimensionless

g = gravitational constant (32.2), ft/sec^2

h = local heat transfer coefficient - Btu/(sq ft)(deg F)(hr)

k = thermal conductivity, Btu/(sq ft)(hr)(deg F/ft)

M = Mach number, u/a, dimensionless

Nu = Nusselt number, hx/k, dimensionless

$\bar{Nu}$ = Nusselt number, referred to isothermal plate conditions

Pr = Prandtl number, $\mu c_p/k$, dimensionless

p = pressure - lbs/in^2

q = heat transfer rate, Btu/hr

$\bar{q}$ = dynamic pressure, $\frac{1}{2}\rho u^2$, lb/in^2

r = temperature recovery factor, dimensionless

Re = Reynolds number, ux/ν, dimensionless

t = temperature, deg F

T = absolute temperature, deg R

u = local velocity in x direction, ft/sec

v = local velocity in y direction, ft/sec

x = distance chordwise from leading edge

y = distance normal to surface

z = distance spanwise

δ = thickness

ϵ = emissivity

γ = ratio of specific heats, c_p/c_v

θ = Sutherland constant

ρ = mass density, lb sec^2/ft^4

σ = Stefan-Boltzmann constant, $(.173 \times 10^{-8})$, Btu/(hr)(sq ft)(deg R)^4

μ = absolute viscosity, lb sec/sq ft

ν = kinematic viscosity, sq ft/sec

ω = viscosity-conductivity temperature exponent, dimensionless,

i.e., $\mu/\mu_o = k/k_o = (T/T_o)^{\omega}$

Subscripts

$()_\delta$ = conditions at edge of boundary layer

$()_e$ = edge conditions

$()_{HM}$ = heat meter

$()_s$ = plate values

$()_o$ = stagnation or reservoir conditions

$()_{aw}$ = adiabatic surface (wall) conditions

$()_w$ = surface (wall) conditions

$()_x$ = local conditions

$()_\infty$ = free stream conditions

$()_{ad}$ = adiabatic rise

$()_{iso}$ = isothermal conditions

I. INTRODUCTION

With the advent of the gas turbine, high speed airplanes, missiles, and rockets, the problem of fluid frictional heating has become critical. From the realization that "aerodynamic heating" can result in an adiabatic surface temperature rise of over 1000°F for a rocket which is at a Mach number of 4, it is evident that from the structural, equipmental, and human standpoint the knowledge of the heat transfer characteristics of such supersonic vehicles is imperative. Since these heat transfer characteristics are associated with the fluid boundary layer, a thorough investigation of the boundary layer, both laminar and turbulent, is necessary in order that the aeronautical designer will have sufficient information to carry out his mission.

The problem of the mechanical and thermodynamical interaction between high speed gas flow and a parallel surface has received considerable study for flows of low Mach number; the results of these investigations for the laminar boundary layer are summarized in Refs. 1 and 2. In the case of heat transfer through the laminar boundary layer on flat plates and cones, for low Mach numbers again, the theory is also quite complete. Refs. 3 and 4 summarize the results of heat transfer at supersonic speeds.

The experimental corroboration, however, of these theoretical results, especially at the higher Mach numbers, is meager. The work of Scherrer and Gowen for a cone at Mach number 2 (Ref. 5), of Eber, also on cones with the Mach numbers ranging from 0.88 to 4.2 (Ref. 6); and of Slack who tested a cooled flat plate at a Mach number of 2.4 (Ref. 7), constitute the bulk of high speed heat transfer research. No attempt

will be made to present their results, since they are nicely summarized in Ref. 4. Also in Ref. 4, Kaye stresses the need for experimental heat transfer coefficients, especially for Mach numbers in excess of 3. This is precisely the problem at hand, the experimental heat transfer from a laminar boundary layer to a cooled flat plate at a nominal Mach number of 5.8.

In undertaking an experimental investigation of this nature, there are always several avenues down which to proceed, and in most cases these avenues lead to blind alleys. This program was no exception. There are also certain decisions which must be made in regard to the scope of the investigation and the methods to be used.

One of these decisions was that of investigating only the laminar boundary layer. It is evident that to evaluate properly the effects of "aerodynamic heating" the turbulent as well as the laminar boundary layer should be investigated. However, due to the stability of the laminar boundary layer at a Mach number of 5.8 and the physical limitations on the model dimensions, it was necessary to limit the investigation to just the laminar layer.

It was also necessary to decide whether to use a heated or a cooled plate. The heated plate had the advantages of better control of surface temperatures and relatively simpler accessories, but since it was necessary to have stagnation or reservoir temperatures in excess of 200°F in order to avoid condensation in the test section, the problems of model construction for surface temperatures of 400°F - 500°F were considerable. Therefore, it was advisable to investigate the direct "aerodynamic heating" problem, i.e., heat transfer to the surface.

A flat plate model was chosen since existing theory predominantly considers this case, and the design requirements of the cooling jacket made such a model more practicable. In addition, the experimentation was coordinated with that of M. Eimer's flat plate skin friction investigation (Ref. 8) which was also carried out in the GALCIT 5 x 5 inch Hypersonic Wind Tunnel.

The scope of the investigation was modest. It was simply to determine experimental heat transfer coefficients of the laminar boundary layer at a nominal Mach number of 5.8 and to compare these coefficients with available theory and other experimental data. However, as a consequence of the investigation, temperature recovery factors were evaluated, and the effect of condensation on heat transfer was noted. In addition, some interesting qualitative results in regard to transition and boundary layer separation are presented.

In summary, this paper presents the results of an experimental investigation in the GALCIT 5 x 5 inch Hypersonic Wind Tunnel, Leg No. 1, of the heat transfer from a laminar boundary layer to a cooled flat plate at a Mach number of 5.8 and the results are compared with available theoretical and experimental data.

II. EXPERIMENTAL EQUIPMENT AND PROCEDURE

A. Description of the Wind Tunnel

All testing was carried out in the GALCIT 5 x 5 inch Hypersonic Wind Tunnel (Leg No. 1), which is of the continuously operating closed return type. The required compression ratios were obtained with five stages of Fuller rotary compressors, and, when necessary, an additional stage of Ingersoll reciprocating compressors. The compressors and all the valving were operated remotely from a master control panel (Cf. Fig. 1) located adjacent to the test section. The air heating system consisted of a multiple pass heat exchanger with superheated steam as the heating medium. The capacity of the system was such that a stagnation temperature of 300°F was obtainable at a stagnation pressure of 94.4 psia.

Oil removal was accomplished by Cyclone separators after each compression stage, finely-divided carbon canisters, porous carbon filter blocks and a Goetz-type molecular filter. The air used during the tests contained approximately 2.5 parts per million (ppm) of oil fog by weight.

Water was removed by a 2200-pound bed of silica gel in the main air circuit, which was reactivated by a built-in blower-heater-condenser system prior to each run. The maximum water content of the air was kept below 100 ppm by weight at all times, the usual value being approximately 22 ppm. The dew point was measured at the beginning and end of each run using a standard type carbon dioxide-cooled indicator.

The tests were conducted at a nominal Mach number of 5.8. The nozzle blocks were designed by the Foelsch method with correction applied for the estimated boundary layer displacement thickness. Static

orifices at one-inch intervals in the top and bottom nozzle blocks permitted a check to be made with the original nozzle calibration on each run.

A 32-tube vacuum-referenced manometer (Cf. Fig. 1) using DC-200 silicone fluid was used to measure all static pressures, and an atmospheric referenced mercury micro-manometer was used to measure the total head pressures. Tunnel stagnation pressure was measured with a Tate-Emery nitrogen-balanced gage and this pressure was controlled within ±.04 psi by means of a Minneapolis-Honeywell Brown circular chart controller.

The stagnation temperature was measured by a thermocouple probe located one inch upstream of the nozzle throat. This temperature was recorded and controlled by means of a Minneapolis-Honeywell Brown circular chart controller. All other temperatures necessary for plant operation were indicated on a 20-point Leeds & Northrup recorder. The overall schematic diagram including the heating system is shown in Fig. 2.

An optical system using a BH-6 steady source was used for the Schlieren or shadow photographs of the flow.

B. Description of the Model

1. General

The model consisted of three components; the stainless steel aerodynamic surface, the heat flow meter, and the brass cooling jacket containing the coolant passageways. These three components with an overall thickness of .65 inches were cemented together with a bonding agent and insulated from the tunnel side walls by 3/16-inch silicone

fiberglass. The model spanned the test section and was supported so that the aerodynamic surface was coincident with the plane of symmetry of the test section. Fig. 3 gives the details of the model while Fig. 4 shows the model mounted in the test section.

2. Aerodynamic Surface

The aerodynamic surface was a 4 5/8-inch wide by 10 inches long by 1/10 of an inch thick stainless steel plate, lapped and polished so that the measured roughness of the plate surface was an average of one microinch from the mean profile. The final polishing was done with 8,000 mesh diamond resulting in a surface emissivity of .070. Ten copper-constantan thermocouples were imbedded .010 of an inch from the upper surface for the purpose of determining the surface temperature. The location and details of the thermocouples are shown on Fig. 5. The 7^{o} leading edge of the aerodynamic surface extended .70 of an inch ahead of the heat meter-radiator assembly. The ten copper-constantan thermocouple wires were insulated from the steel plate by fiberglass cloth cemented to the lower side of the surface. A bakelite terminal strip attached to the aft edge of the plate permitted the attachment of heavier thermocouple wires which were connected to the leads from the measuring instrument by means of a leak-tight Cannon plug mounted in the tunnel wall. Fig. 6 shows the details of this connection. Three orifices, at $2\frac{1}{2}$, 5, and 8 inches from the leading edge, for the purpose of giving surface static pressures were also installed in the aerodynamic surface. These orifices were located 1 inch off the centerline of the plate.

3. Heat Flow Meter

The heat flow meter (Cf. Ref. 9) consisted of three 4 5/8 inches wide by 9 inches long by 1/64 inch thick bakelite sheets laminated together. The central sheet contained nineteen (19) 1/2 inch by 1 inch thermopile elements. In addition, two copper-constantan thermocouples were installed for the purpose of determining the heat meter temperature. The location of each thermopile element is given in Fig. 7. A bakelite terminal strip was attached to the aft edge of the heat meter and provided a means of connecting the heavier leads from the measuring instrument. These leads passed through the tunnel wall in the same manner as the surface thermocouple leads (Cf. Fig. 6).

The thermopile element consists of a series of thermocouples which are positioned so that one set of junctions ("hot junctions") is in a plane adjacent and parallel to one face of the heat meter while the other set of junctions ("cold junctions") is placed adjacent and parallel to the opposite face of the heat meter. Heat flow through the meter will now generate an electromotive force due to the difference in temperature between the "hot" and "cold" junctions of the thermopile. By calibration of the thermopile elements from a known heat source, the heat flux in Btu/hr - ft^2 will be represented by a known voltage across the "hot" and "cold" junctions.

The thermopile is constructed by winding (about 120 turns) No. 40 constantan wire onto a bakelite core. This is then silver-plated over one-half of the coil, which results in each junction between the plated and unplated wire acting as a thermocouple. In this way a large number

of thermocouples connected in series is obtained. Therefore, a small variation in temperature across each element will represent a substantial e.m.f. The elements are then inserted into the cut-outs in the center lamination, connected to the copperwires leading to the heat meter terminal strip, and cemented between the top and bottom cover sheets of the heat meter. Fig. 7 gives the details of the construction of a typical thermopile element.

4. Cooling Jacket

The cooling jacket containing the coolant passageways was fabricated from brass sheet screwed and cemented to the side and center stiffeners. It was designed so that the coolant entered the upper section through fittings in the tunnel wall. The coolant is then channeled both chordwise and spanwise by means of baffle plates to holes in the center plate, allowing the fluid access to the lower section exit passageways. The details of the cooling jacket and the fittings in the tunnel walls are shown in Figs. 3 and 6.

C. Test Equipment and Instrumentation

1. Temperature Measurements

In addition to the ten (10) thermocouples measuring the surface temperature of the plate and the two (2) thermocouples in the heat meter, two (2) copper-constantan thermocouples were installed in the upper surface of the tunnel test section. These temperatures were used in computing the radiant heat transfer to the cooled plate from the heated tunnel wall. Also recorded were the inlet and exit temperatures of the

coolant by means of thermocouples attached to the cooling system piping. All these temperatures were measured on a 48-point Minneapolis-Honeywell Brown Electronic self-balancing potentiometer (Cf. Fig. 1) with a range of -100°F to 500°F and an accuracy of ±1°F.

2. Heat Transfer Measurements

Since each thermopile element in the heat meter was calibrated in Btu/(hr - sq ft - millivolt) it was sufficient, in order to obtain heat transfer rates, to measure the millivolt output of each element. These voltages were measured on a 24-point Minneapolis-Honeywell Brown Electronic self-balancing potentiometer (Cf. Fig. 1). The instrument was equipped with ranges from 0 to 10 mv and 0 to 25 mv with an accuracy of ±.02 mv and ±.05 mv respectively.

3. Cooling System

The coolant used for the tests was water obtained from the compressor plant cooling system. The return line from the cooling towers on the roof of the Guggenheim Aeronautical Laboratory was connected to a twenty-five gallon atmospheric reservoir adjacent to the tunnel test section. The level of this reservoir was controlled by a ball-type float valve. From the reservoir, the water passed through a Sarco water blender which was also connected to the building hot water system. By adjustment of the water blender, the temperature of the water entering the model could be controlled to ±1°F. From the water blender the coolant passed through the tunnel walls and model to the inlet port of an ECO Engineering close-coupled PP-2M positive displacement pump which

pumped the fluid back into the compressor plant system for cooling. The pumping rate through the model was 600 g.p.h.

By connecting the model on the suction side (25 inches of Hg.) of the pump, the pressure differential between the model cooling jacket and the test section, while the tunnel is running, was approximately five psi. This feature permitted the use of the thin sheeted cooling jacket. However, in order to protect the model from high differential pressures due to a pump failure, a second ECO pump was installed as a stand-by in parallel with the first. The second pump was controlled by means of a Minneapolis-Honeywell Vacuumstat mercury switch which switched on its motor if the model internal pressure rose above 22 inches of Hg. A schematic of the cooling system is shown in Fig. 8, while Fig. 9 gives various details of the system.

For the case of the zero heat transfer runs, when no coolant was used, the internal pressure of the model was reduced by by-passing the flow directly into the pump, but still leaving the model connected to the suction side.

D. Test Procedure

1. Calibration of Heat Meter

Since the e.m.f. per degree and the distance between the thermopile junctions are unknown, the thermal conductivity of the bakelite lamination uncertain, and the conductivity along the wire also unknown, the heat meter assembly must be calibrated.

The uni-directional heat flow apparatus used to calibrate the heat meter was similar to that described in Ref. 10 and an "exploded"

sketch of the components is shown in Fig. 10. Nichrome ribbon (.010") is welded into a heating element and cemented to the surface of a heat meter. The heat meter and the thin heating element are then cemented on to a heating plate which is used as a guard heater. A very thin sheet of silicone fiber glass is placed over the heating element to electrically insulate the nichrome ribbon from the surface of the model. This assembly is then placed on top of the flat plate model, which includes the heat meter that is to be calibrated, and the entire "sandwich" securely clamped together.

When the temperature of the thin heating plate is equal to the temperature of the guard plate, the heat meter between the two heaters will indicate zero output. This means that all the heat from the heating plate is either transferred through the heat meter to the cooling element or lost from the edges. The edge loss is a function of the edge area A, the convective conductance, f_c, and the temperature difference between the edge surface and the surrounding air, Δt.

By adjusting the energy input and the cooling water rate, it is possible to bring the heat meter very close to room temperature. Taking the maximum temperature difference allowed between the model surface-heat meter assembly and the air to be $5^{\circ}F$, the maximum error due to edge losses can be calculated. The edge loss, q_e, may be expressed as

$$q_e = f_c A \Delta t \qquad (1)$$

In this case, f_c is approximately one, A is .03 sq. ft. and Δt is the order of five, giving an edge loss of approximately 0.15 Btu/hr. The heat supplied to the meter being calibrated is about 60 Btu/hr. Thus,

if the edge loss is completely ignored, the resulting error will be in the order of 0.30 per cent. If the temperature of the heat meter is kept constant and the heat rate through the meter is varied, the edge loss from the meter will be a function of the temperature of the meter and will remain constant; therefore, the percentage error due to edge loss will be very small if the heat rate through the meter is very large.

The power input to the nichrome heater was measured by a wattmeter and the output of the heat meter elements by means of the Brown self-balancing potentiometer. An average of several readings was used to calculate the calibration constant of each thermopile. The greatest source of error is probably due to the non-uniform contact resistance between the heating assembly and the model.

Table I gives the calibration constants of the heat meter elements at a heat meter temperature of 120°F. Fig. 11 gives the conversion constant for other heat meter temperatures.

2. Heat Transfer Runs

Since a fixed nozzle block was used during the investigation, only a small variation in Mach number was possible. This resulted in having temperature and pressure as the only controllable parameters. In addition, due to the design of the cooling system, it was advisable to hold the temperature of the coolant constant. Therefore, the runs were made under various combinations of stagnation (reservoir) temperature and pressure.

The procedure for each heat transfer run was that the stagnation temperature (t_o) was held constant and the stagnation pressure (p_o)

varied from its maximum (100 psig) to the lowest value at which flow could be maintained (45 psig). The ranges of p_o and t_o were as follows:

	p_o - psig.			
t_o °F	45	60	80	100
	--	--	195	--
	215	215	215	215
	225	--	--	--
	245	245	245	245
	--	265	265	265
	--	285	285	285

The lower range of stagnation temperatures were for the purposes of investigating the influence of condensation.

In order to obtain equilibrium conditions, it was necessary to run for a period of approximately 2 hours before data could be taken. This equilibrium condition was considered reached when the temperatures from the thermocouples installed in the model and the test section, and the output of the thermopile elements in the heat meter reached a nearly constant value. After each change in stagnation pressure, an additional steadying period was necessary. Upon reaching equilibrium, all temperatures and heat meter outputs were recorded. At the same time the model and tunnel wall static pressures were also taken.

3. Insulated (Zero Heat Transfer) Runs

In order to calculate the heat transfer coefficient (h) from the equation

$$q/A = h\,(T_w - T_{aw}) \qquad (2)$$

it is necessary to have, in addition to the wall temperature and heat

transfer rate, the "adiabatic wall temperature" (T_{aw}). By definition this temperature is the temperature the plate would reach if it were insulated. (i.e., $(\partial T/\partial y)_{y=0} = 0$) To obtain this temperature, the model cooling system was bypassed and the same combination of stagnation temperatures and pressures as for the heat transfer runs were repeated. Upon reaching equilibrium the model surface temperatures represented (T_{aw}). In most of the runs, zero heat transfer, as indicated by the heat meter output, was not possible so the adiabatic wall temperatures were obtained by interpolating and extrapolating the data to the condition of zero heat transfer.

III. THEORY

Since the theory of the laminar boundary layer on a flat plate with zero pressure gradient is well known, it will not be repeated in this paper. However, for completeness, a summary of the laminar boundary layer equations with some of their solutions, as well as the equations of heat transfer, are given in Appendix A.

The justification that the boundary layer approximations are valid for flows at Mach number 6 is given by Li and Nagamatsu in Ref. 11 and by Lees in Ref. 12.

IV. DISCUSSION OF RESULTS

A. Pressure and Mach Number Distribution on Flat Plate Model

1. Pressure Distribution

The surface pressure ratio distribution p/p_o obtained from the plate static pressure orifices is shown for the case of a stagnation pressure of 95.5 psia and a stagnation temperature of 265°F on Fig. 12. This distribution is representative of the various combinations of stagnation pressures and temperatures. The maximum variation in pressure ratio is .04 which for the case shown is 1.5% per inch over the after portion of the plate; however, the variation is much less over the forward portion. This is typical of the runs at the higher stagnation pressures and can be the result of the rear orifice being in the transition region. Also shown in Fig. 12 is the distribution of $p/\sqrt{q}$ which has about the same percentage variation as p/p_o.

2. Mach Number Distribution

The distribution of Mach number along the plate is also shown on Fig. 12. The maximum variation of Mach number is .06 or 1.03%. Thus, theoretical results for flat plates should apply since the local free-stream Mach number, or velocity, is essentially constant.

B. Surface Temperature and Heat Transfer Rates

1. Surface Temperatures

Four surface temperature distributions in °F are presented in

Fig. 13 for stagnation pressures of 115.5, 95.5, 75.5, and 60.4 pounds per square inch absolute. The stagnation temperatures varied from 285°F for a stagnation pressure of 115.5 psia to 225°F for a stagnation pressure of 60.4 psia. These are representative of all the data obtained. Fig. 13(a) shows data for conditions such that the boundary layer appears to be laminar up to about $7\frac{1}{2}$ inches where the beginning of transition is indicated by a sudden rise in surface temperature and heat transfer rate. On Fig. 13(d) the indication is that the position of transition has moved downstream to about the 9-inch station. This is shown more graphically, later, in the presentation of the heat transfer coefficients. Examination of the temperature distribution shows that over the first third of the plate the temperature decreases with nearly a constant gradient, while over the center third of the plate the value of the wall temperature is nearly constant, but possessing a second derivative with respect to length. Over the last two inches of the plate the values of the temperature increase and the first derivative also is variable.

In addition to the temperature distribution having second derivatives with respect to the chordwise distance, at the higher stagnation pressures and temperatures, the spanwise temperature distribution on the after portion of the plate also has second derivatives with respect to the spanwise distance (Cf. Fig. 14). The forward portion of the plate, on the other hand, is practically isothermal spanwise. This appears to be due to the contamination of the surface by the tunnel sidewall boundary layer which raises the surface temperatures near the tunnel walls and increases with distance chordwise. The existence of these second derivatives in temperature is important, since they represent an

adjustment that must be applied to the measured heat transfer rates due to conduction in the surface plate.

2. Heat Transfer Rates

The heat flow rate into a unit area of the heat meter, for steady state conditions, is given by the equation

$$\left(q/A\right)_{HM} = h\left(T_w - T_{aw}\right) - K_s \delta_s \left(\frac{\partial^2 T}{\partial x^2} + \frac{\partial^2 T}{\partial z^2}\right) - \text{Radiation} \qquad (3)$$

The first term on the right side of the equation represents the convective heat transfer from the boundary layer. Appendix A gives the derivation of this relationship. The second term represents the heat flow due to conduction in the surface plate, k_s and δ_s are the thermal conductivity and thickness of the surface plate respectively. The third term represents the heat due to radiation from the test section walls and upper nozzle block.

Since the heat flow rate represented by Eq. 3 is the value measured by the heat flow meter, the subtraction of the last two terms must be made in order that the heat transfer coefficient can be properly evaluated.

In order that the conduction term can be written as shown and not as an integral, the assumption is that $\partial T/\partial y$ is constant across the thickness of the surface plate. This appears valid since the plate is thin and the amount of heat being transferred is such that $\partial T/\partial y$ is small. The chordwise temperature gradient was constant over the first third of the plate, so the conduction term is zero. Over the second third of the plate, the contribution was primarily due to the derivative $\partial^2 T/\partial x^2$, while over the last third of the plate, the contribution was

due to both $\partial^2 T/\partial x^2$ and $\partial^2 T/\partial z^2$. Over the last third of the plate this adjustment became as large as 20 per cent of the heat transferred. The effect of heat conduction in the heat meter is negligible, since the heat meter thickness is less than half the thickness of the surface plate, and the thermal conductivity of the meter material (bakelite) is .134 Btu/hr - ft - ^{o}F as compared to the stainless steel surface plate whose thermal conductivity is 9.4 Btu/hr - ft - ^{o}F. This means that for the same temperature variation, the value of heat transferred due to conduction in the heat meter is less than 1% of the heat transferred from the surface plate.

The heat transferred due to radiation from the nozzle blocks and tunnel walls may be calculated from the equation from McAdams (Ref. 13) which for this particular case is

$$q/A = - \frac{\sigma(T_1^4 - T_2^4)}{\frac{1}{\bar{F}_{12}} + \left(\frac{1}{\epsilon_1} - 1\right) + \left(\frac{1}{\epsilon_2} - 1\right)} \qquad (4)$$

where σ is the Stefan-Boltzmann constant = .173 x 10^{-8} Btu/ft^2 - hr (^{o}R)^4

ϵ_1 is emissivity of model surface = .07

ϵ_2 is emissivity of nozzle block = .13

$\bar{F}_{12}$ is factor for position of two parallel walls = .85

T_1 is model surface temperature ^{o}R

T_2 is nozzle block surface temperature ^{o}R

Due to the heat transfer through the test section nozzle block, the surface temperature of the block never exceeded 150^{o}F. So for the extreme case of T_1 = 540^{o}R and T_2 = 610^{o}R the heat transfer due to radiation was q/A = 2.75 Btu/hr - ft^2 which is less than 1% of the heat

transferred for this condition. Therefore, the radiation effects were neglected.

Thus, only the contribution due to conduction must be computed and subtracted. The q/A distributions resulting are shown in Fig. 13. These distributions are representative of all the data.

C. Temperature-Recovery Factors

1. Evaluation of Temperature Recovery Factor

The average experimental heat transfer rates adjusted for the conduction term are presented in Fig. 15 as a function of the ratio of surface temperature to stagnation temperature for four values of stagnation pressure. For each position along the plate, the data points are located very nearly as a straight line. This indicates that, for the range of surface temperature and stagnation temperatures involved, the heat transfer coefficients are independent of the surface temperature or the temperature potential causing the heat transfer. Due to the greater heat transferred to the bottom of the model, it was possible to obtain negative (heat transferred from the plate to the fluid) heat transfer rates for every thermopile element except at the 9.45-inch station. This permitted the immediate determination, except at the 9.45-inch-station, of the T_w/T_o ratio for the condition of zero heat transfer. For the case of the 9.45-inch station the resulting curve had to be extrapolated to the zero heat transfer condition.

Knowing the ratio of T_{aw}/T_o, the recovery factor can be calculated from the equation

$$r = 1 - \frac{T_o - T_{aw}}{T_o}\left[\frac{2}{(\gamma-1)M_\delta^2} + 1\right] \qquad (5)$$

Fig. 16 presents the temperature recovery factors as a function of Reynolds number. This Reynolds number is based on the distance from the leading edge of the plate and on air properties evaluated at the free stream static temperature. Fig. 17 gives the Reynolds number per inch, and Fig. 18 the air properties (Cf. Ref. 14) used throughout the computations. The data indicate that the temperature recovery factor for the laminar boundary layer is essentially a constant value of 0.858 $\pm$ .004 up to a Reynolds number of 1.2×10^6. For the transition zone which extends from a Reynolds number of 1.2 to 2.2 million, the recovery factors exhibit considerable scatter. The apparent cause of this scatter will be explained in a subsequent section on transition.

2. Correlation with Theory and Other Experimental Data

In the usual treatment of laminar boundary layer theory, an assumption is made to the effect that the Prandtl number is independent of the temperature of the fluid. By this assumption, the temperature recovery factor can be closely approximated by $Pr^{1/2}$. For the present investigation the value of the $Pr^{1/2}$ varies from .862 to .832 when based on the free stream and the average adiabatic wall temperatures respectively. In reality, some intermediate temperature should be the basis of the Prandtl number evaluation, but this temperature cannot be explicitly determined from the existing theories. The present experimental value for the recovery factor lies between $Pr_\delta^{1/2}$ and $Pr_{aw}^{1/2}$, though closer

to $Pr_{\delta}^{1/2}$. This result of r = .858 may be slightly high, in that it appears from review of other experimental data (see below) that the adiabatic wall temperature has the greater influence when evaluating the Prandtl number.

On comparing the experimental value with other experiments conducted at lower Mach numbers the agreement is favorable. Wimbrow, Stone, and Scherrer, des Ches and Sternberg, and Eber, testing cones up to a Mach number of 4.5, have recovery factors lying between 0.845 and 0.855. The Massachusetts Institute of Technology tested a flat plate and also obtained a recovery factor of 0.85. However, Slack, and also Stalder, Rubesin and Tendeland, testing flat plates at a Mach number of 2.4 found recovery factors of 0.88, which is somewhat high in face of the previous evidence. All the above data are summarized in Ref. 4.

Therefore, it appears that the present investigation confirms the laminar recovery factor of 0.85, and extends its range of Mach number independence up to a Mach number of 5.8. This is also predicted theoretically for hypersonic Mach numbers in Ref. 15. Also substantiated is the independence of the laminar recovery factor on Reynolds number up to the beginning of transition of the laminar boundary layer.

D. Heat Transfer Results

1. Evaluation of Heat Transfer Coefficients

The heat-transfer coefficients calculated from the experimental data are presented in Fig. 19. The calculations were made from Eq. 2

$$q/A = h (T_w - T_{aw})$$

These results were obtained from tests at 115.5, 95.5, 75.5, and 60.4 psia stagnation pressures and stagnation temperatures varying from 225°F to 285°F. For the run at 60.4 psia, the boundary layer was laminar over nine inches of the plate and the heat-transfer coefficients decreased in value with increasing distance along the plate. At the nine inch station the heat-transfer coefficients begin to increase with increasing distance giving indication of the beginning of transition. With an increase in stagnation pressure, the position at which transition begins moves upstream, and at a stagnation pressure of 115.5 psia it is near the $7\frac{1}{2}$-inch station. This is consistent with the temperature recovery factor data. However, the temperature recovery plot indicates transition begins slightly ahead of the $7\frac{1}{2}$-inch station, but the agreement is within the range of the experimental accuracy. Since the heat transfer coefficient is a function of Reynolds number, the scatter of the experimental data can be partially attributed to the varying Reynolds numbers resulting from covering a range of stagnation temperatures at each stagnation pressure.

2. Correlation with Theory and Other Experiments

In Appendix A, it is shown that the local heat transfer coefficients in dimensionless form can be related to local skin friction by the expression

$$Nu/Re^{1/2}\ Pr^{1/3} = c_f\ Re^{1/2}/2 \qquad (6)$$

If the data are presented as $Nu/Re\ Pr^{1/3}$ as a function of Reynolds number, a correlation with other skin friction and heat transfer results is possible. Fig. 20 presents the experimental data in this form and they are

compared with other experimental and theoretical curves from Refs. 8 and 16. These dimensionless representations are of general value only for results obtained from a surface with a uniform temperature. The present results, however, are obtained from a surface that is not isothermal so cannot be compared directly. In order to make the proper correlation, the present results must be related to the case of the uniform temperature plate.

Two methods for effecting this correlation were investigated. One was that given by Chapman and Rubesin in Ref. 16 and the other was that of Lighthill in Ref. 17. The Chapman-Rubesin method required that the temperature distribution be expressed in a power series in distance along the plate. This was rather difficult to accomplish for the distributions measured. Lighthill's method, on the other hand, reduced to a problem of numerical integration which was easily computed. Fig. 20 gives a representative curve of the ratio of the heat transfer coefficient with a temperature distribution to the heat transfer coefficient of an isothermal plate as a function of the chordwise distance along the plate. Also shown, for comparison, is the same ratio computed from the method of Chapman and Rubesin, where the surface temperature was expressed as a fourth degree polynomial. The agreement is good over the center portion but diverges over the leading and trailing portions of the plate. In each case the temperature at the leading edge of the plate is considered as the adiabatic temperature. This assumption is reasonable, since the plate is uncooled at the leading edge, and an extrapolation of the measured temperature data to the leading edge checks very closely with the adiabatic value. Appendix A presents the complete expressions

used in determining the Lighthill relationship.

Fig. 22 presents the heat-transfer correlation from Fig. 20 as related to the case of an isothermal plate. The scatter of the data is within $\pm 10\%$ of the value $Nu/Re^{1/2}\ Pr^{1/3} = 0.285$. This checks, within the scatter, with Eimer's (Ref. 8) skin friction measurement of $c_f\ Re^{1/2}/2 = 0.270$ made at the same Mach number of 5.8. This agreement is very good in that his results were for an insulated plate $T_w/T_\delta = 6.4$ while the heat transfer case is for $T_w/T_\delta \approx 6.2$. This value, however, is 10% below that of Chapman and Rubesin (Ref. 16) computed on the basis of the viscosity used in the present investigation. At a Reynolds number of 1.6 million the beginning of transition is indicated by the sharp increase in $Nu/Re\ Pr^{1/3}$ which was as indicated in the curves of heat transfer coefficients. All the air properties were based on free stream static temperature.

The results then indicate that, within accuracy of the experiments, the relationship between heat transfer and skin friction as predicted by the laminar boundary layer theory is valid at a Mach number of 5.8.

E. Additional Results

1. Transition

As previously discussed, the experimental data indicate that a transition from the laminar boundary layer begins in the Reynolds number range of 1.2 - 1.5 million. This is below the results of a preliminary investigation carried out in the GALCIT 5 x 5 inch Hypersonic Wind Tunnel,

on a long flat plate. Testing this 28-inch plate at approximately the same Reynolds and Mach numbers, there was no indication of natural transition at the 10-inch station. The method of transition indication was by means of fluorescent lacquer. Therefore, some explanation is required for the present data.

Examination of the photograph of the model, (Fig. 4) shows that a shroud cover beginning at the ten-inch station and extending downstream is installed. Prior to installing this cover plate, the wake off of the thermocouple and heat meter terminal blocks, and from the leads themselves, was of such magnitude that supersonic flow in the tunnel could not be established. The addition of the cover reduced the turbulence to such a degree that supersonic flow was possible. The thickness of the shroud, however, resulted in an increase (.065") in the model thickness at the ten-inch station, and it is this step in thickness which may cause the transition. It is believed that the shock wave, associated with the flow deflection over this step, interacts with the laminar boundary layer causing some transition upstream. This effect, however, needs further investigation before it can be positively stated that such is the case. Notwithstanding the cause of the transition, the present investigation shows that the use of the heat meter as a transition indicator is excellent. It is small, rugged, extremely sensitive, and can be used for conditions where pressure measurements are not feasible.

2. Condensation Effects on Heat Transfer

An attempt was made to determine the effect of condensation on the heat transfer coefficients. Runs were made at a stagnation tem-

perature just below the condensation-free temperature and then were repeated at a temperature just above the condensation-free temperature. Within the accuracy of the measurements, there was no difference in the heat-transfer coefficients. However, the ratio of T_w/T_o for zero heat transfer was 2% lower for the case with condensation than without condensation. This is partially substantiated by the analysis of Ref. 8.

3. Flow Separation

In reducing the stagnation pressure in order to make runs at lower Reynolds numbers, it was noted that at a pressure of about 42 psig there was a sharp increase in surface static pressures and the heat transfer rate. Investigation, by means of the Schlieren system, showed that at these lower pressures, a separation of the laminar boundary layer from the surface of the plate was occurring. Fig. 23 presents the Schlieren photographs of the boundary layer just before and after separation.

A review of the other experimental data provides a clue to the cause of this separation. From the heat-transfer coefficient curve (Fig. 19), it can be seen that a reduction in stagnation pressure results in a downstream movement of the transition region. At a stagnation pressure of 45 psig (60.4 psia), the beginning of transition has moved almost to the end of the plate. By further reducing the stagnation pressure, the transition point seems to move to the junction of the surface plate and the cover shroud. Now if the pressure is lowered below this value, and if the transition point trys to move up over the cover plate, the presence of the adverse pressure gradient associated with the flow over

the junction may be of such magnitude that a separation results.

When the flow separated, there was a rapid increase in the heat transfer rate and the surface static pressures. This increase becomes as large as 300% in both cases. The condition after separation (Fig. 23(b)) was extremely stable, and the boundary layer could not be reattached to the plate unless the stagnation pressure was increased to over 60 psig.

Due to the model configuration and its mounting in the tunnel it was not possible to investigate this problem completely at the present time. However, it seems to be of sufficient interest that further study is warranted.

V. CONCLUSIONS

The present investigations provided the following evidence as to the behavior of the heat transfer characteristics of the laminar boundary layer at a Mach number of 5.8:

1. The heat transfer coefficient (h) computed from the Newtonian equation $q/A = h\ (T_w - T_{aw})$ is independent of the temperature potential causing the heat transfer.

2. The temperature recovery factor for the laminar boundary layer was .858 which, when compared to the bulk of previous experiments, extends the range of Mach number independence of the temperature recovery factor to a Mach number of 5.8. The laminar recovery factor being independent of the Reynolds number up to the beginning of transition was also substantiated.

3. The heat transfer coefficients obtained with a negative chordwise temperature gradient can be as much as 60% higher than the coefficients resulting from a surface at constant temperature.

4. Heat transfer results when referred to the case of an isothermal plate give a value of .285 for the non-dimensional heat transfer parameter $\overline{Nu}/Re^{1/2}\ Pr^{1/3}$, the estimated accuracy of this result being $\pm 10\%$. When compared to the theory and to the skin friction experiments made at the same Mach number, the theoretical relationship of $Nu/Re^{1/2}\ Pr^{1/3} = c_f\ Re^{1/2}/2$ appears valid for the laminar boundary layer heat transfer at a Mach number of 5.8.

The investigation also provided some evidence as to:

1. The possibility of forcing transition at a comparatively low (1.2×10^6) Reynolds number by the presence of a shock-wave boundary layer interaction.

2. The effect of condensation on the temperature recovery factor, which it lowered, and on the heat transfer coefficients, which remained unchanged.

3. The separation of the boundary layer, which occurred when the transition point was subjected to an adverse pressure gradient, and which was extremely stable once it had occurred.

REFERENCES

1. Rubesin, M. W. and Johnson, H. A.: "A Critical Review of Skin Friction and Heat Transfer Solutions of the Laminar Boundary Layer of a Flat Plate". Trans. ASME, Vol. 71, No. 4, May 1949, pp. 383-388.

2. Kuerti, G.: "The Laminar Boundary Layer in Compressible Flow". Advances in Applied Mechanics. ed. R. von Mises and T. von Kármán, Vol. II, Academic Press, Inc., New York, N. Y., 1951.

3. Johnson, H. A. and Rubesin, M. W.: "Aerodynamic Heating and Convective Heat Transfer-Summary of Literature Survey". Trans. ASME, Vol. 71, No. 5, July 1949, pp. 447-456.

4. Kaye, Joseph: "Survey of Friction Coefficients, Recovery Factors, and Heat Transfer Coefficients for Supersonic Flow". Presented at the 21st Annual Meeting of the Institute of the Aeronautical Sciences, Jan. 26-29, 1953.

5. Scherrer, Richard and Gowen, Forrest E.: "Comparison of Theoretical and Experimental Heat Transfer on a Cooled 20° Cone with a Laminar Boundary Layer at a Mach Number of 2.02". NACA TN 2087, 1950.

6. Eber, G. R.: "Recent Investigations of Temperature Recovery and Heat Transmission on Cones and Cylinders in Axial Flow in the Naval Ordnance Laboratory Aeroballistics Wind Tunnel". Journ. Aero. Sci., Vol. 19, No. 1, Jan. 1952, pp. 1-7.

7. Slack, Ellis G.: "Experimental Investigation of Heat Transfer Through Laminar and Turbulent Boundary Layers on a Cooled Flat Plate at a Mach Number of 2.4". NACA TN 2686, 1952.

8. Eimer, M.: "Experimental Skin Friction at Hypersonic Mach Numbers". Ph.D. Thesis, California Institute of Technology, Pasadena, California, 1953.

9. Martinelli, R. C.; Morrin, E. H.; and Boelter, L. M. K.: "An Investigation of Aircraft Heaters. V - Theory and Use of Heat Meters for the Measurement of Rates of Heat Transfer Which Are Independent of Time". NACA ARR, Dec. 1942.

10. University of California, Department of Engineering: N-7-ONR-295 Task I. Thermal Radiation Project - Final Report - Series 10, Sept. 1, 1950.

11. Li, Ting-Yi and Nagamatsu, H. T.: "Shock Wave Effects on the Laminar Skin Friction of an Insulated Flat Plate at Hypersonic Speeds". Contract No. DA-04-495-Ord-19, Memorandum No. 9, July 1, 1952, California Institute of Technology, Pasadena, California.

12. Lees, Lester: "On the Boundary Layer Equations in Hypersonic Flow and Their Approximate Solutions". ADRC Contract No. AF 33(038)-250 Report No. 212. Princeton University, Sept. 20, 1952.

13. McAdams, W. H.: "Heat Transmission", McGraw-Hill Book Co., Inc., New York, 1942.

14. Keyes, F. G.: "The Heat Conductivity, Viscosity, Specific Heat, and Prandtl Numbers for Thirteen Gases". Massachusetts Institute of Technology, April 1, 1952, United States Navy and United States Air Force, Project Squid Technical Report 37.

15. Probstein, R. F. and Lees, L.: "On the Recovery Factor for Hypersonic Flow with a Self-Induced Pressure Gradient". Princeton University Engineering Laboratory, Report No. 217, Jan. 19, 1953.

16. Chapman, Dean R. and Rubesin, Morris W.: "Temperature and Velocity Profiles in the Compressible Laminar Boundary Layer with Arbitrary Distribution of Surface Temperature". Journ. Aero. Sci., Vol. 16, No. 9, Sept. 1949, pp. 547-565.

17. Lighthill, M. J.: "Contributions to the Theory of Heat Transfer Through a Laminar Boundary Layer". Proc. Roy. Soc., Series A, Math and Phys. Sci., No. 1070, 7 August 1950, Vol. 202, pp. 359-377.

18. Lewis, J. A.: "Monograph V, Boundary Layer in Compressible Fluid". AMC-T2 Technical Report F-TR-1179-ND, Feb. 1948.

19. von Kármán, Th. and Tsien, H. S.: "Boundary Layer in Compressible Fluids". Journ. Aero. Sci., Vol. 5, Feb. 1938.

20. Brainerd, J. G. and Emmons, H. W.: "Effect of Variable Viscosity on Boundary Layers, with a Discussion of Drag Measurements". Journ. of Applied Mechanics, Vol. 9, A-1, March 1942.

21. Crocco, Luigi: "Boundary Layer of Gases Along a Flat Plate". Rend. Mat. Univ. Rome, V., Vol. 2, p. 138, 1941. (University of California Engineering Projects Translation by George Lowenkerg, edited by M. W. Rubesin, Oct. 17, 1947.).

22. Hantzsche, W. and Wendt, H.: "The Laminar Boundary Layer of the Flat Plate with and without Heat Transfer and Considering Compressibility". Jahrbuck 1942 det Deutschen Luftfahrtforschung, Part I, pp. 40-50. (University of California Engineering Projects Translation by Ronald Kag, edited by M. W. Rubesin, May 1, 1947.)

23. Cope, W. F. and Hartree, D. R.: "The Laminar Boundary Layer in Compressible Flow". Philos. Trans. Roy. Soc., London, Series A, Vol. 241, pp. 1-69, 1948.

24. Van Driest, E. R.: "Investigation of the Laminar Boundary Layer in Compressible Fluids Using the Crocco Method". Aerophysics Laboratory Report AL-1183, North American Aviation, Inc., Jan. 9, 1951.

25. Young, G. B. W. and Janssen, E.: "The Compressible Boundary Layer". Journ. Aero. Sci., Vol. 19, No. 4, p. 229, April 1952.

26. Moore, L. L.: "A Solution of the Laminar Boundary Layer Equations for a Compressible Fluid with Variable Properties, Including Dissociation". Journ. Aero. Sci., Vol. 19, No. 8, p. 505, August 1952.

27. Eckert, E. and Weise, W.: "The Temperature of the Unheated Bodies in a High Speed Gas Stream". NACA TM 1000, Jan.-Feb., 1941.

28. Eckert, E.: "Heat Transmission of Bodies in Rapidly Flowing Gases". Intelligence T-2, Air Documents Office, Foreign Exploitation Section, Wright Field, Dayton, Ohio, 1946.

29. Goldstein, G. (editor): "Modern Developments in Fluid Dynamics". Oxford University Press, England, Vol. 2, 1938, pp. 627-631.

30. Conforto, F.: "The Integration of a System of Equations Relating to the Theory of the Boundary Layer in Gases". Seminario Matenatico Rendiconte, University of Roma, Rome, Italy, Vol. 2, 1941.

31. Eckert, E. and Drewitz, O.: "Heat Transfer to a Plate in Flow at High Speed". NACA TM 1045, May-June 1943.

32. Michels, W. C.: "Advanced Electrical Measurements". D. Van Nostrand Co., Inc., New York, 2nd ed., 1941, Ch. 1.

APPENDIX A

SUMMARY OF THE LAMINAR BOUNDARY LAYER AND HEAT TRANSFER EQUATIONS

A. Boundary Layer Equations for Flat Plate

1. General Formulation of Problem

Convective heat transfer like fluid (skin) friction is considered a boundary-layer phenomenon, and it is assumed that the heat passes to the fluid by molecular conduction through a laminar layer which is always present immediately on the surface for a continuum region.

No attempt will be made to derive the boundary layer equations in this paper, as the derivation of these equations are well known and can be found in many references. However, the general problems and the historical progress in the solutions of these equations will be presented for the purpose of completeness.

The characteristics of the laminar boundary layers of temperature and velocity for an infinitely thin flat plate placed parallel to the fluid stream are found by the simultaneous solutions to the following conservation of mass, momentum, and energy equations, which are for the case of no pressure gradient along the plate, i.e., $\partial p/\partial x = 0$.

$$\frac{\partial}{\partial x}(\rho u) + \frac{\partial}{\partial y}(\rho u) = 0 \tag{A-1}$$

$$\rho u \frac{\partial u}{\partial x} + \rho v \frac{\partial u}{\partial x} = \frac{\partial}{\partial y}\left(\mu \frac{\partial u}{\partial y}\right) \tag{A-2}$$

$$\frac{\partial p}{\partial y} = 0$$

$$\rho u \frac{\partial}{\partial x}(C_p T) + \rho v \frac{\partial}{\partial y}(C_p T) = \frac{\partial}{\partial y}\left(K \frac{\partial T}{\partial y}\right) + \mu \left(\frac{\partial u}{\partial y}\right)^2 \tag{A-3}$$

with the boundary conditions

$x < 0$	$y \geq 0$	$u = u_\infty$	$T = T_\infty$
$x \geq 0$	$y = 0$	$u = 0, v = 0$	$T = T_w$ or $\left(\frac{\partial T}{\partial y}\right)_w = 0$
$x \geq 0$	$y \to \infty$	$u = u_\infty$	$T = T_\infty$
$x \to -\infty$	$y \geq 0$	$u = 0, v = 0$	$T = T_w$ or $\left(\frac{\partial T}{\partial y}\right)_w = 0$

(i.e., assumption of infinitely thick boundary layers at $x \to -\infty$.) These equations are the result of applying the boundary layer approximations to the complete conservation of mass, momentum, and energy equations. The justification that these approximations are valid for flows at Mach number 6 are given by Li and Nagamatsu and by Lees in Refs. 11 and 12.

It will be noticed from the manner in which the equations are written that ρ, μ, k, and c_p may vary throughout the region of integration, thus making the equations perfectly general for the case of zero pressure gradient along the plate. The second term of the right member of Eq. (A-3) is that which accounts for the dissipation of mechanical energy into thermal energy by the viscous forces prevailing in the boundary layer.

The nature of these equations and the boundary conditions are such that a certain similarity exists with respect to a variable made up of terms such as y/x^m, where m is a positive constant. The boundary conditions remain the same whether by variation of x and y, the variable approaches zero or infinity, also it reduces the partial differential equations to total differential equations which can then be integrated. An excellent review of the mathematics of the various solutions to these equations is given by J. A. Lewis in Ref. 18.

2. Solutions to the Boundary Layer Equations

A summary of the solutions of the laminar boundary-layer equations for a flat plate in compressible (air) flow, taking into account the temperature variation due to conduction and frictional heating is given by Rubesin and Johnson in Ref. 1. In general these analyses always assumed a constant value of Prandtl number and an approximate expression for the viscosity variation with temperature. Thus, the applicability to a wide Mach number range is questionable. von Kármán and Tsien in Ref. 19 treated both the insulated plate and the heat transfer cases with Mach number as high as 10. They assumed Prandtl number invarient with temperature and viscosity exponents of 0.76.

Brainerd and Emmons (Ref. 20) examined the insulated plate case with Mach numbers up to 3.16 and used Pr = 0.733 and ω = 0.768. Crocco (Ref. 21) obtained solutions for both insulated plate and heat transfer cases, assuming Pr = 0.725 and ω = 1.5, 1.00, .75, and .50. Hantzsche and Wendt (Ref. 22) also treated the insulated plate and heat-transfer cases with Mach number up to 10. They examined two combinations of air properties: optional Prandtl number and ω = 1.0, and optional ω and Pr = 1.0. Cope and Hartree (Ref. 23) used Pr = 0.76, ω = 0.89 in their investigations.

More recently using Crocco's method of hand calculation, Van Driest (Ref. 24) obtained results for Pr = 0.75 and a Sutherland law of viscosity-temperature variation, θ = 0.505, for the heat transfer plate and the insulated plate with a constant value of specific heat at constant pressure assumed. Young and Janssens (Ref. 25) and Moore (Ref. 26)

solved the reduced boundary layer equations in integral form using a differential analyzer with the experimental values of air properties. Moore also included dissociation at higher temperatures.

B. Heat Transfer Equations

In Ref. 3, Johnson and Rubesin summarize the equations for the heat transfer of the laminar boundary layer; however, again for completeness, these equations will be included. The following presentation of the development of the heat transfer equations is essentially that of Ref. 3.

1. Newtonian Heat Transfer Equation

In the usual treatment, the heat rate is taken as proportional to the temperature difference between the surface and the ambient fluid. Thus, the rate of convective heat transfer is

$$q/A = -K\left(\frac{\partial T}{\partial y}\right)_{y=0} = \bar{h}(T_w - T_\delta) \tag{A-4}$$

with the heat-transfer coefficient being defined as

$$\bar{h} = \frac{-K\left(\partial T/\partial y\right)_{y=0}}{(T_w - T_\delta)} \tag{A-5}$$

where T_w = wall temperature

T_δ = free stream temperature

A = area

2. Nusselt Number

However, for the purposes of correlating the heat-transfer data

in dimensionless form, Eq.(A-5) is written in terms of the Nusselt number.

$$Nu = \frac{\bar{h}x}{K} = \frac{-\left(\frac{\partial T}{\partial y}\right)_{y=0}}{(T_W - T_\delta)/x} \tag{A-6}$$

Using this definition, Refs. 27 and 28 show that from the steady-flow energy of a fluid and for a given geometrical system that

$$Nu = f_1 \left[Re, Pr, M, \Delta T_{ad}/(T_W - T_\delta) \right] \tag{A-7}$$

Of the five dimensionless variables in Eq. (A-7), only three, Nu, Re, and Pr, normally appear for heat transfer since M and $\Delta T_{ad}/(T_W - T_\delta)$ are substantially zero for low velocity flow. Consequently, the Nusselt number and in turn the heat transfer coefficient h, are independent of the temperature potential $(T_W - T_\delta)$ which is a necessary requirement in order that Eq. (A-4) may conveniently represent the rate of heat transfer. At high velocities, however, the temperature factor $\Delta T_{ad}/(T_W - T_\delta)$ in Eq. (A-7) is finite, and Nu is dependent on the temperature potential, thereby destroying the usefulness of Eq. (A-4).

3. Modified Temperature Potential

In order to deduce a heat-transfer equation in which the temperature potential and heat-transfer coefficient are independent, consider the following:

Suppose that an insulated plate is placed in a high velocity stream, the rate of heat flow and consequently the temperature gradient with respect to the normal to the surface must be zero. Pohlhausen in Ref. 29 has shown that the resulting temperature distribution is such

that the temperature of the fluid adjacent to the plate exceeds the free stream value. The temperature which the plate (and the fluid in contact with the plate) assumes is designated as the "adiabatic surface temperature", T_{aw}.

If the plate is heated or cooled, then the temperature of the plate will differ from the adiabatic temperature; and since heat is being transferred to or from the fluid, the temperature gradient with respect to the normal is no longer zero.

It is logical then to express the convective heat transfer with frictional heating by

$$q/A = h\,(T_w - T_{aw}) \qquad \text{(A-8)}$$

where h = heat transfer coefficient with frictional heating

$(T_w - T_{aw})$ = modified temperature potential

In order to establish the usefulness of Eq. (A-8), it is necessary to investigate the relationship between the adiabatic surface temperature and the coefficient h.

4. Recovery Factor

Considering T_{aw} first, it can be seen from Eqs. (A-6) and (A-7) that when the plate is insulated, i.e., $T_w = T_{aw}$ and $(\partial T/\partial y)_{y=0} = 0$, Eq. (A-7) reduces to

$$\frac{T_{aw} - T_\delta}{\Delta T_{ad}} = \frac{T_w - T_\delta}{T_o - T_\delta} = \frac{T_{aw} - T_\delta}{u_e^2/2 g C_p} = f_2(R_c, P_r, M) \qquad \text{(A-9)}$$

or defining the temperature difference ratio as the "recovery factor" r

$$r = \frac{T_{aw} - T_{\delta}}{u^2/2gC_p} \qquad \text{(A-10)}$$

A knowledge of the recovery factor r is then a necessity to the determination of the modified temperature potential $(T_w - T_{aw})$ and is treated independently of the heat transfer.

For laminar flow along a flat plate, the recovery factor has been evaluated analytically by several authors (Refs. 21, 22, and 29) and these results show that the recovery factor is independent of Reynolds number and Mach number, for the range in Mach number where disassociation is not present, and is well represented by

$$r = Pr^{1/2} \qquad \text{(A-11)}$$

Because the Prandtl number was maintained as an independent parameter in the various solutions, no means of determining the reference temperature at which to evaluate Pr is possible from these solutions. However, the numerical solutions of Crocco-Conforto (Ref. 30) showed that for Pr = 0.725 the recovery factor was 0.85. Young and Janssan in Ref. 26 showed that the recovery factor has a value of .851 and .841 for a Mach number of 4.23 and 6.42 respectively, with the ambient temperature being 100°R.

5. Convective Heat Transfer Coefficient with Frictional Heating h

The heat-transfer coefficient with friction h has been investigated theoretically for laminar flow over flat plates in Ref. 31 and it was shown conclusively that it is independent of the modified temperature potential and is identical with that for low speeds as evaluated for the

same Reynolds and Prandtl number, i.e., $h = \bar{h}$.

6. Relationship between Nusselt Number and Friction Coefficient

The expression for the relationship between the local Nusselt number and the local friction coefficient is

$$Nu_x = \frac{h_x X}{K} = \frac{C_{f_x}\sqrt{Re_x}}{2} P_r^{1/3} Re_x^{1/2} \qquad \text{(A-12)}$$

where the subscript x refers both to a characteristic length x, measured along the length of the plate from the leading edge, and to local values of all quantities represented in the equation. All of the properties, including density in the defining equation of local friction, are based on the same temperature. The derivation of Eq. (A-12) is given in Ref. 1.

7. Heat Transfer with a Surface Temperature Distribution

Most theories consider only the case of a plate with a constant surface temperature; however, Chapman and Rubesin (Ref. 16) and Lighthill (Ref. 17) treat the problem of a variable surface temperature. In Chapman and Rubesin's analyses the surface temperature is expressed as a power series in the plate length parameter x. Lighthill on the other hand does not make this restriction.

Since most experimental results are for the non-isothermal plate, it is necessary to refer these results to the isothermal case before a proper correlation with most of the theoretical solutions can be made. The method used in this investigation was that of Lighthill's. The expressions used are as follows:

For the flat plate, Lighthill's solution (with the constant multiplier reduced 2 per cent) is:

$$q/A = -.332\left(\frac{u}{\nu x}\right)^{1/2} P_r^{1/3} K \int_{\xi=0}^{x} \frac{d\left[T_w(\xi) - T_{aw}\right]}{\left[1-\left(\xi/x\right)^{3/4}\right]^{1/3}} \qquad \text{(A-13)}$$

which for the case of T_w = constant, reduces to

$$q/A = -.332\left(\frac{u}{\nu x}\right)^{1/2} P_r^{1/3} K\,(T_w - T_{aw}) = h\,(T_w - T_{aw}) \qquad \text{(A-14)}$$

and

$$(T_w - T_{aw}) = 0 \qquad \text{for} \qquad \xi = 0$$

Since we define the Nusselt number as

$$Nu = \frac{(q/A)\,x}{K(T_w - T_{aw})}$$

The ratio of the heat transfer with a temperature distribution to the heat transfer for an isothermal surface can be expressed as

$$\frac{Nu}{Nu_{iso}} = \frac{h}{h_{iso}} = \left[\int_{\xi=0}^{x} \frac{d\left[T_w(\xi) - T_{aw}\right]}{\left[1-\left(\xi/x\right)^{3/4}\right]^{1/3}}\right] \Big/ (T_w - T_{aw}) \qquad \text{(A-15)}$$

So, from the temperature distribution on the surface, the ratio of the heat transfer rates reduces to a problem in numerical integration. Fig. 21 shows a representative chordwise distribution of this ratio.

APPENDIX B

EXPERIMENTAL ACCURACY AND REPEATABILITY

The estimate of the accuracy of the final results is based on the accuracy and repeatability of the individual measurements. The estimated maximum error or repeatability of the individual measurements is as follows:

Measurement	Estimated Maximum Error	Basis of Estimate
Static Pressure - p	.4 mm of silicone	Reading Error
Stagnation Pressure - p_o	less than 1%	Calibration of Tate Emery Gage
Stagnation Temperature - T_o	$\pm 2^{\circ}F$	Calibration of T_o Probe
Surface Temperature - T_w	$\pm 1\frac{1}{2}^{\circ}F$	Calibration of Model
Heat Transfer Rate - q/A	$\pm 5\%$	Maximum Spread of Calibration Data
Adiabatic Wall Temperature - T_{aw}	$\pm 3\frac{1}{2}^{\circ}F$	Accuracy of Temperature Measurements and Spread of q/A Data

The accuracy of computed values based on the errors of the individual measurements is as follows. These values were computed by the method given in Ref. 32.

Quantity	Calculated Error
M	less than 1%
Re	1%
Recovery Factor - r	$\pm$.01
Heat Transfer Coefficient - h	
Forward Portion of Plate	$\pm$13%
Center and Rear Portion of Plate	$\pm$10%
$Nu/Re^{1/2}\ Pr^{1/3}$	
Forward Portion of Plate	$\pm$13%
Center and Rear Portion of Plate	$\pm$10%

TABLE I

HEAT METER CALIBRATION CONSTANTS

(Btu/sq. ft. - hr. - mv. at 120°F)

No.	Constant	No.	Constant	No.	Constant
1	58	6	54	15	--
		7	43		
2	62	8	43	16	86
		9	41		
3	72	10	58	17	98
		11	58		
4	55	12	50	18	60
		13	63		
5	50	14	49	19	68

LIST OF FIGURES

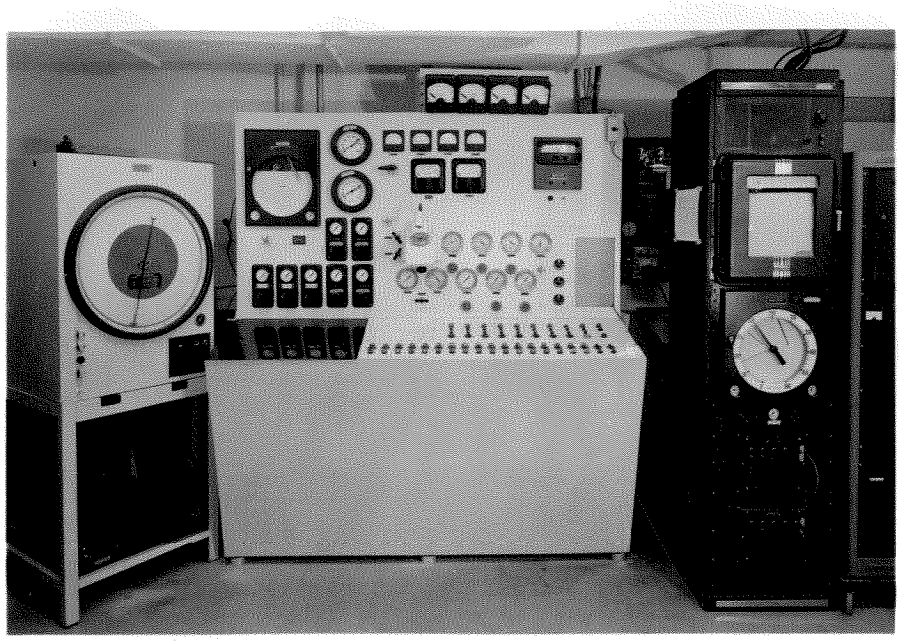

Compressor Plant Motor and Valve Controls
Reservoir Pressure and Temperature Regulators
Plant Pressure and Temperature Indicators

Fig. 1a

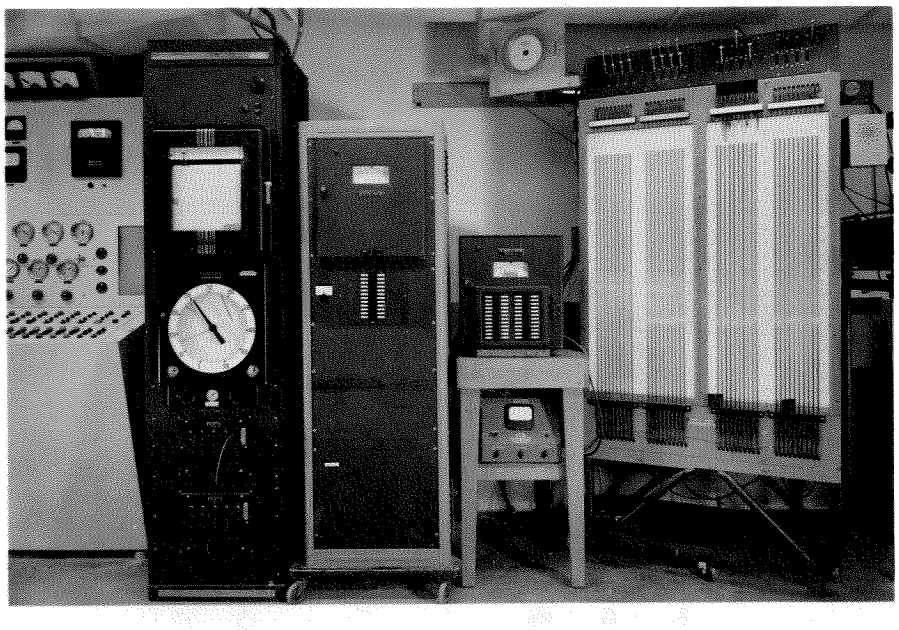

Test Section and Nozzle Block
Pressure and Temperature Instrumentation

Fig. 1b

GALCIT 5 x 5 IN. HYPERSONIC WIND TUNNEL
CONTROLS AND INSTRUMENTATION

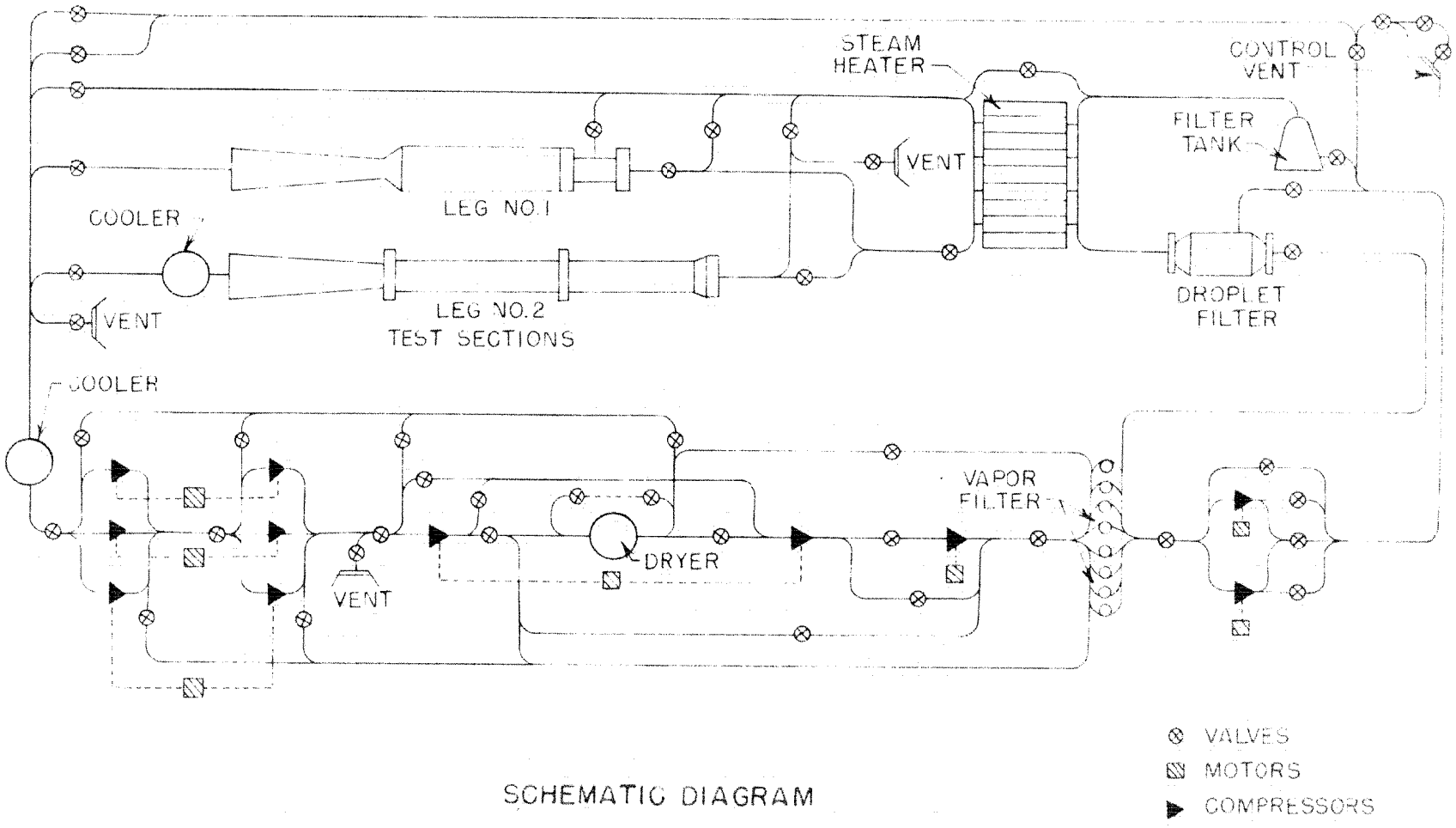

SCHEMATIC DIAGRAM

OF GALCIT 5x5in HYPERSONIC WIND TUNNEL INSTALLATION

FIG.2

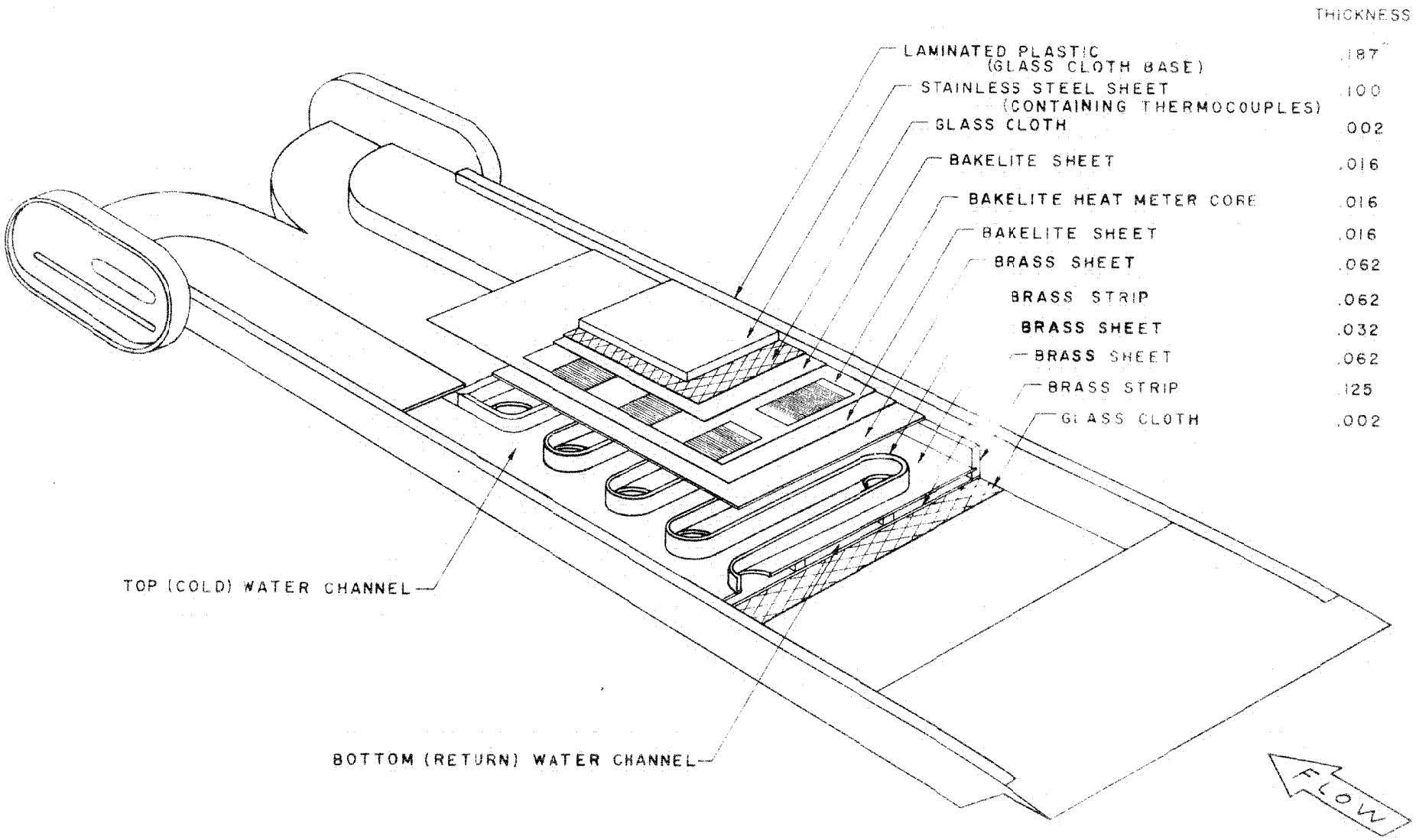

FIG. 3 HEAT TRANSFER MODEL

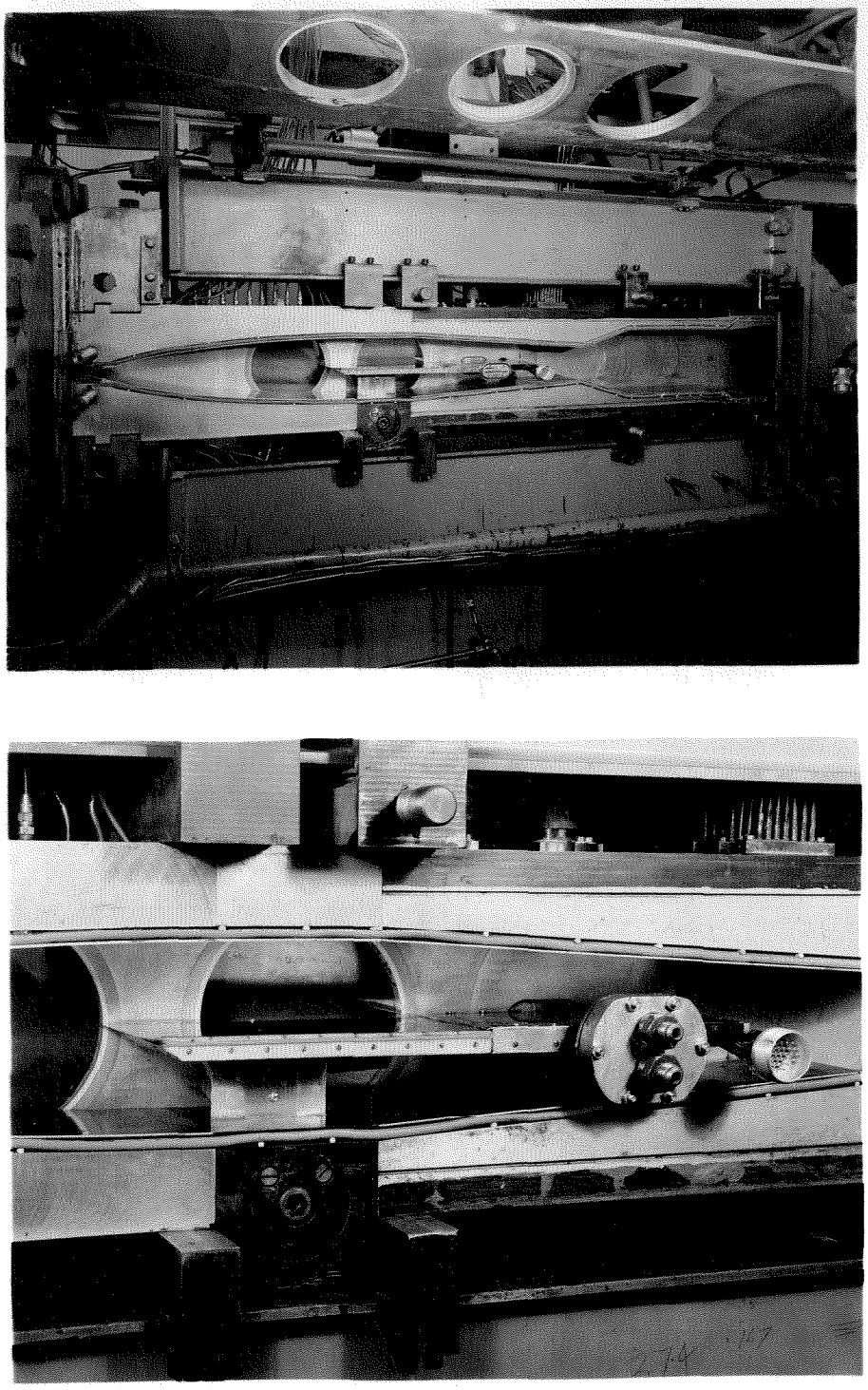

Fig. 4

Flat Plate Heat Transfer Model in Test Section

of GALCIT 5" x 5" Hypersonic Wind Tunnel

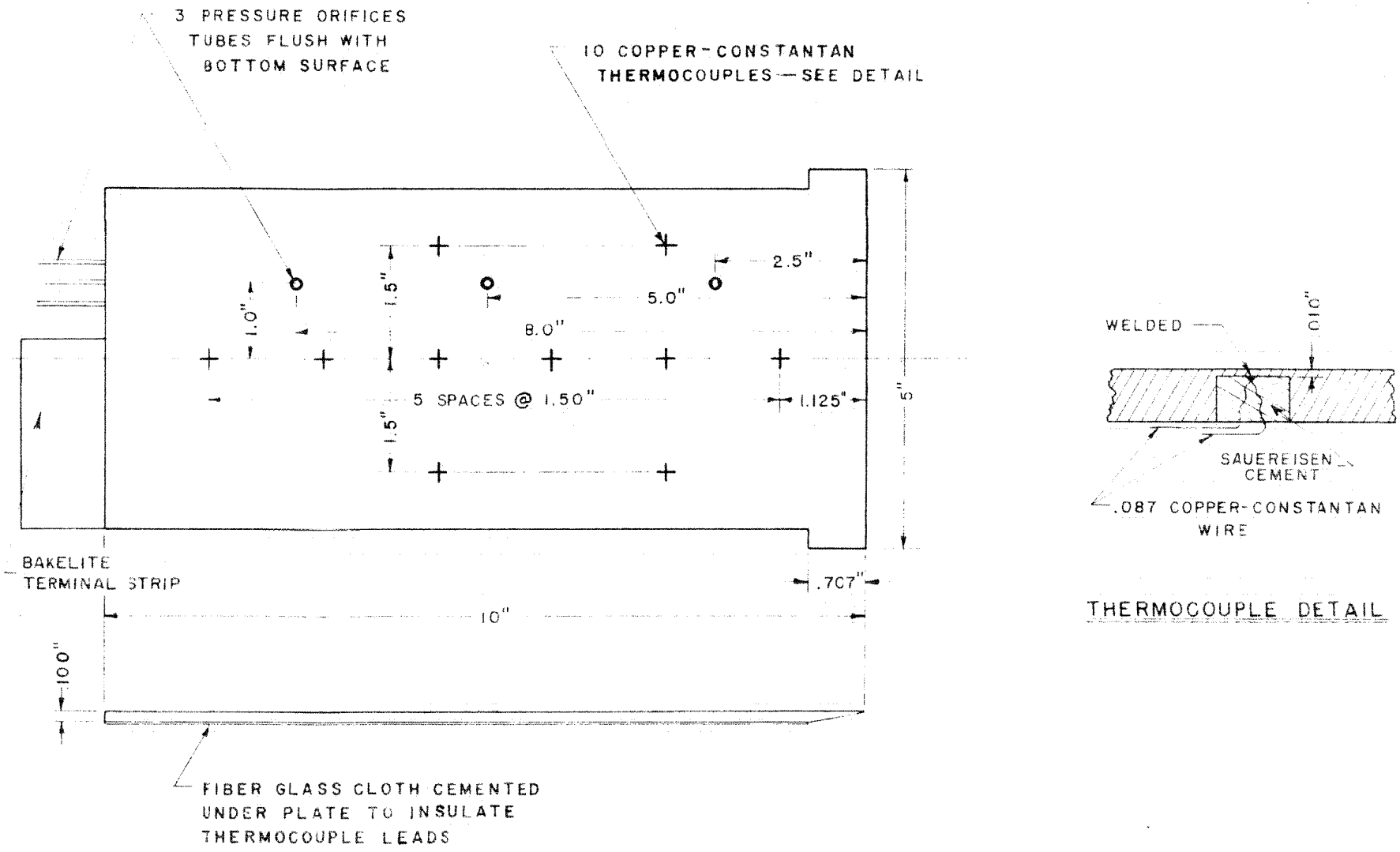

FIG. 5 SURFACE THERMOCOUPLE AND PRESSURE ORIFICE LOCATIONS

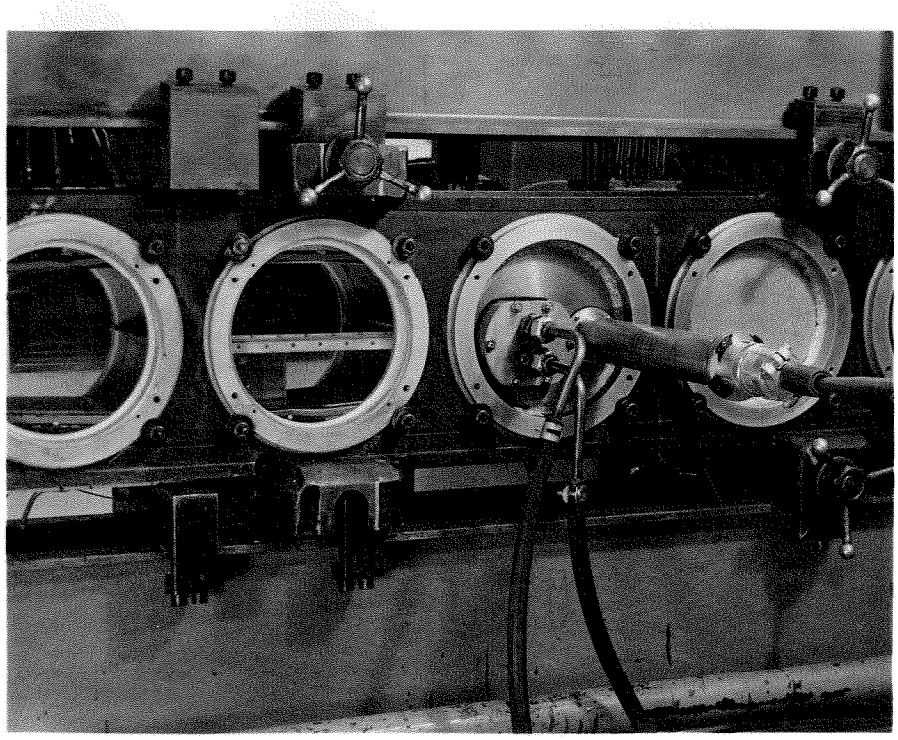

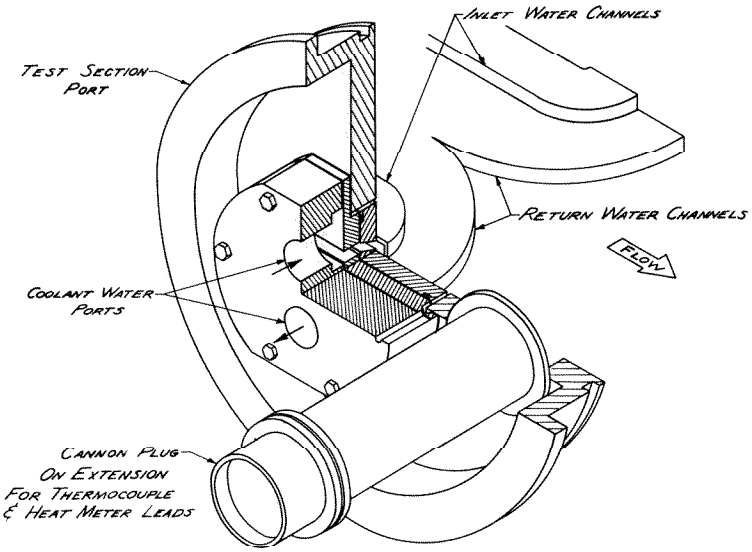

Fig. 6

Details of Tunnel Wall Fittings for Coolant and Electrical Leads

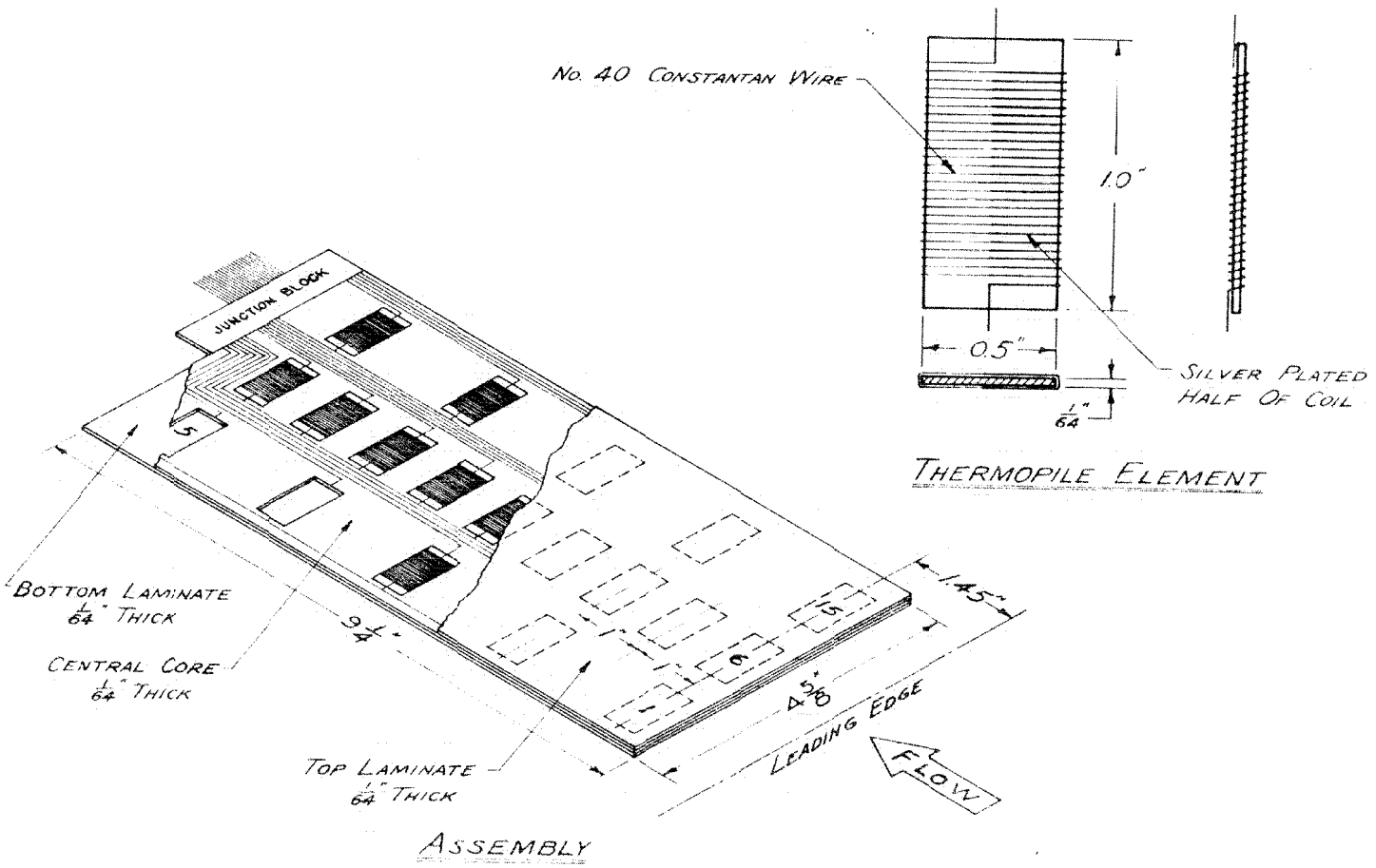

FIG. 7 HEAT METER

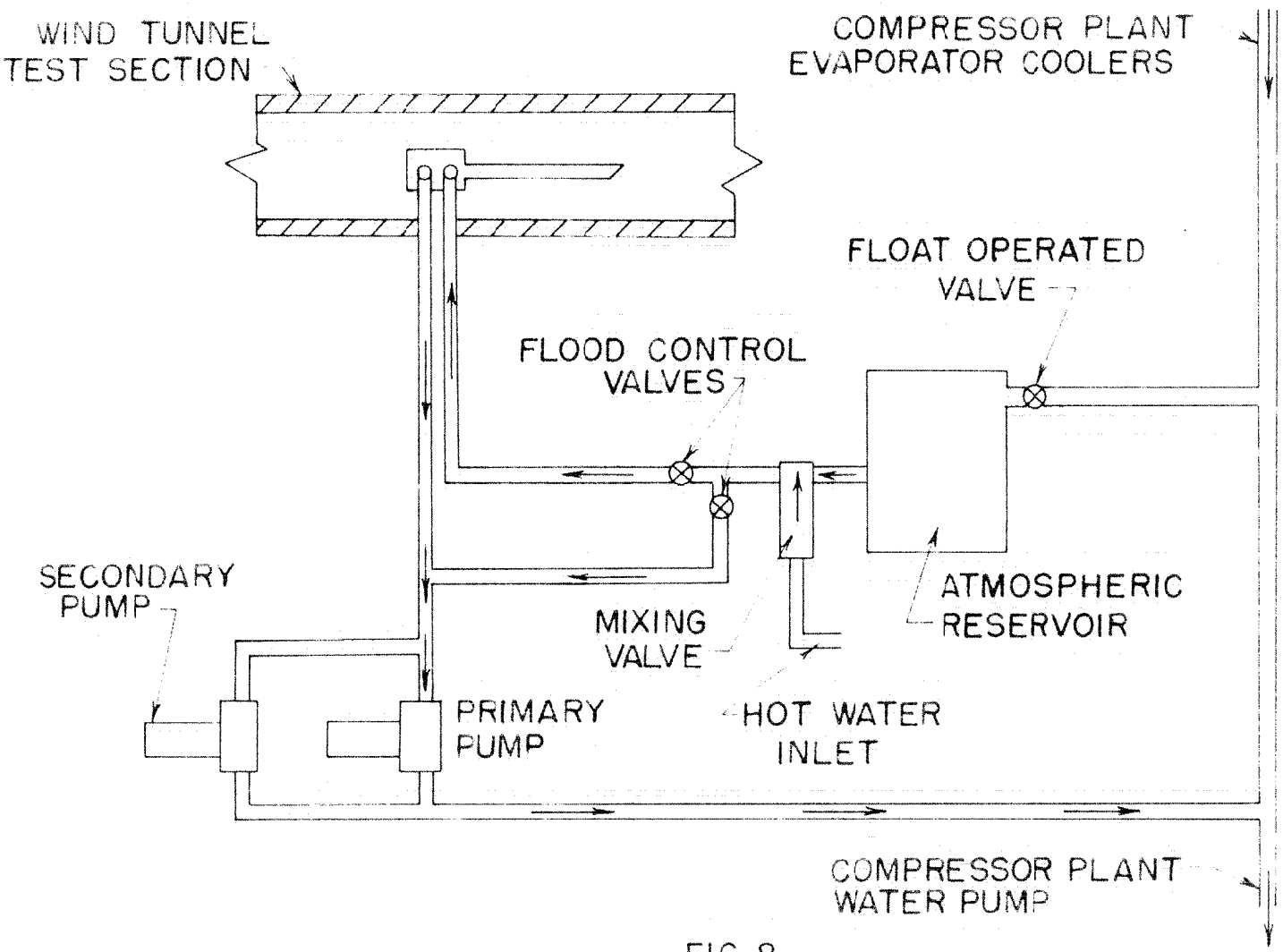

FIG. 8
SCHEMATIC DIAGRAM
OF WATER COOLING SYSTEM

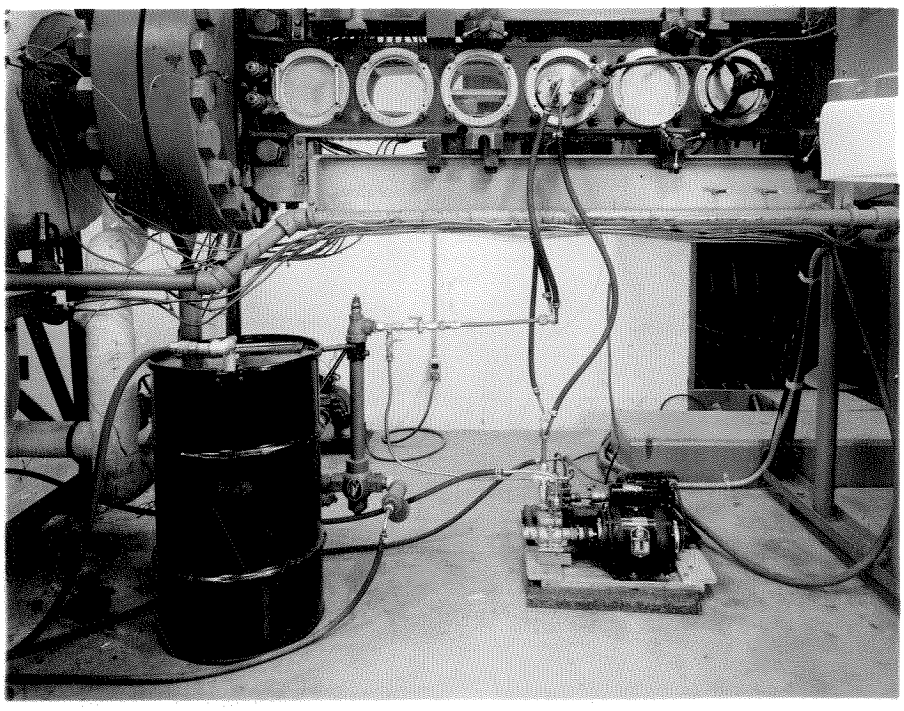

Fig. 9

Cooling System for Heat Transfer Model

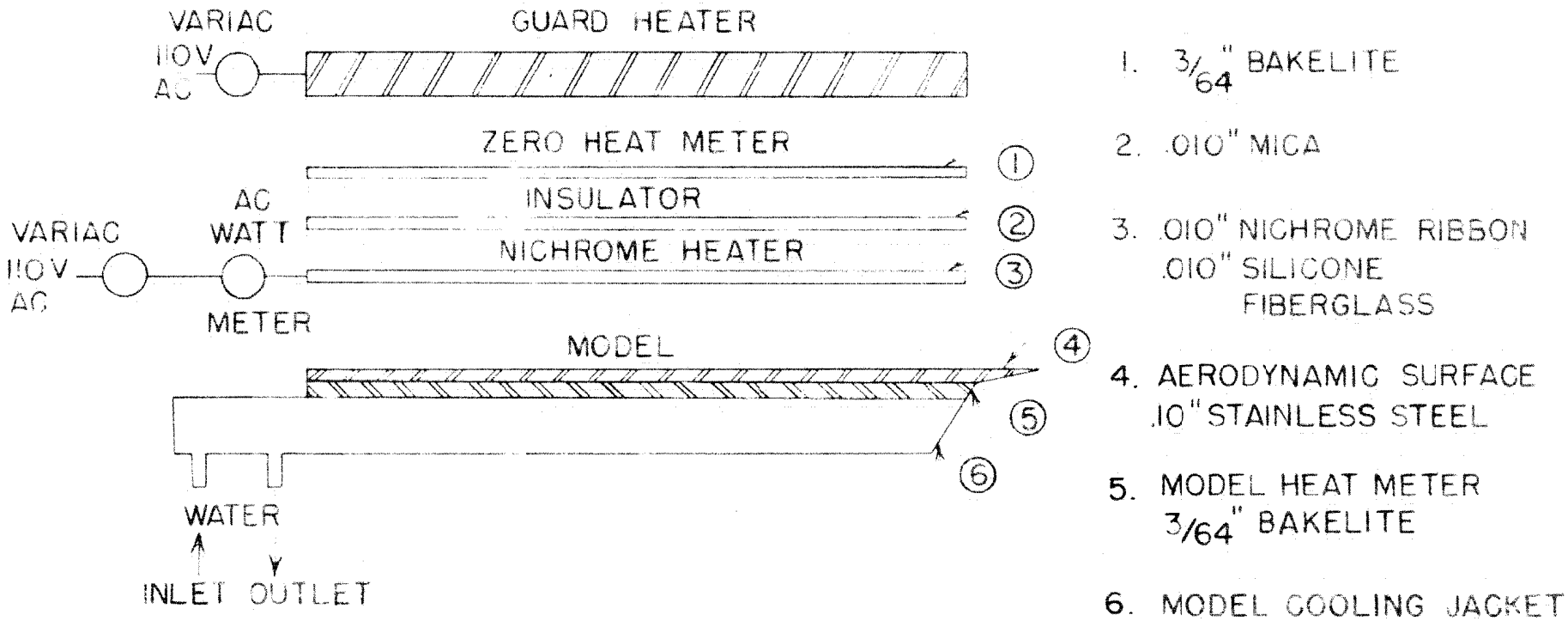

FIG. 10

EXPLODED DIAGRAM

UNIDIRECTIONAL HEAT METER CALIBRATION STAND

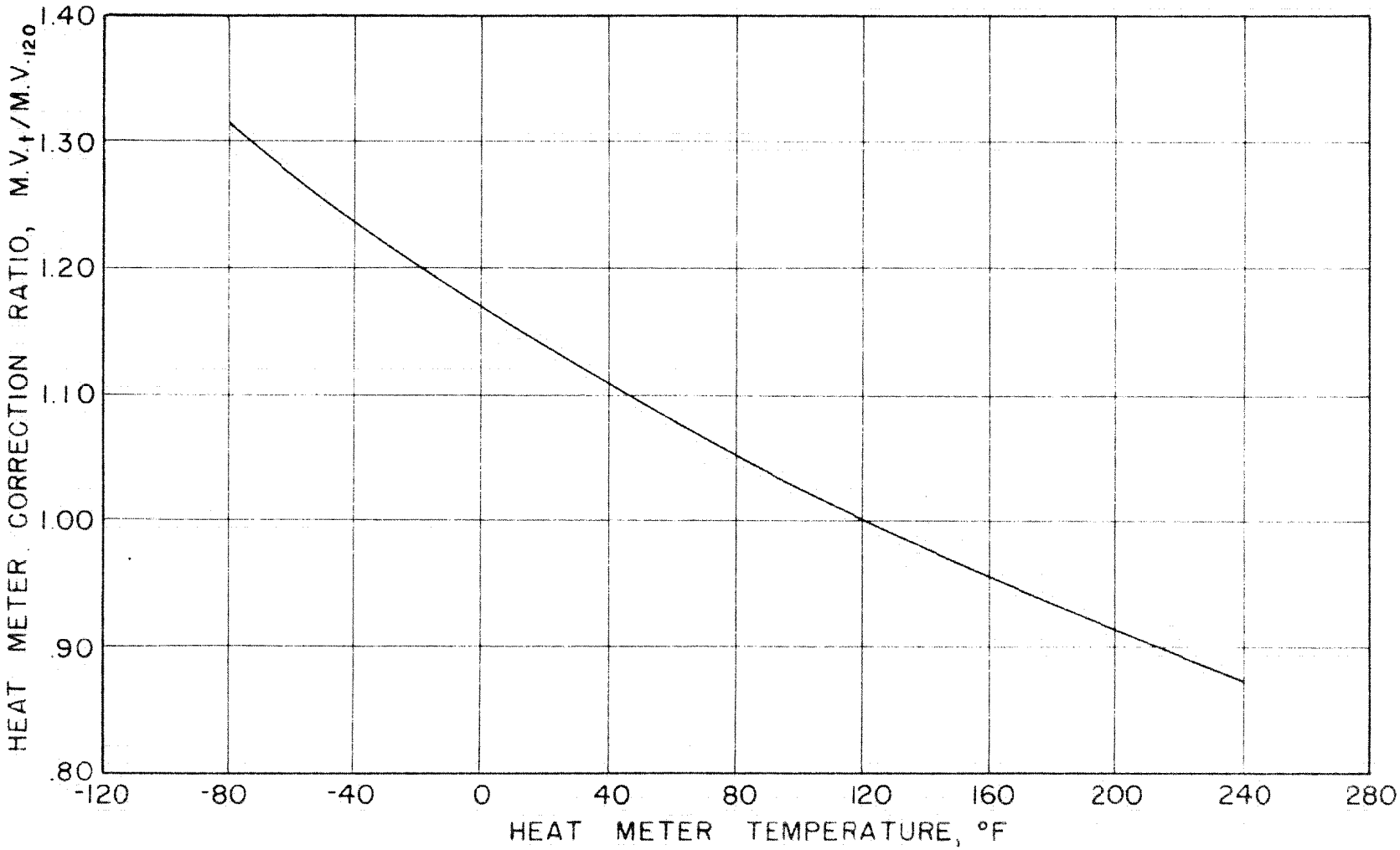

FIG. 11 HEAT METER TEMPERATURE CORRECTION RATIO

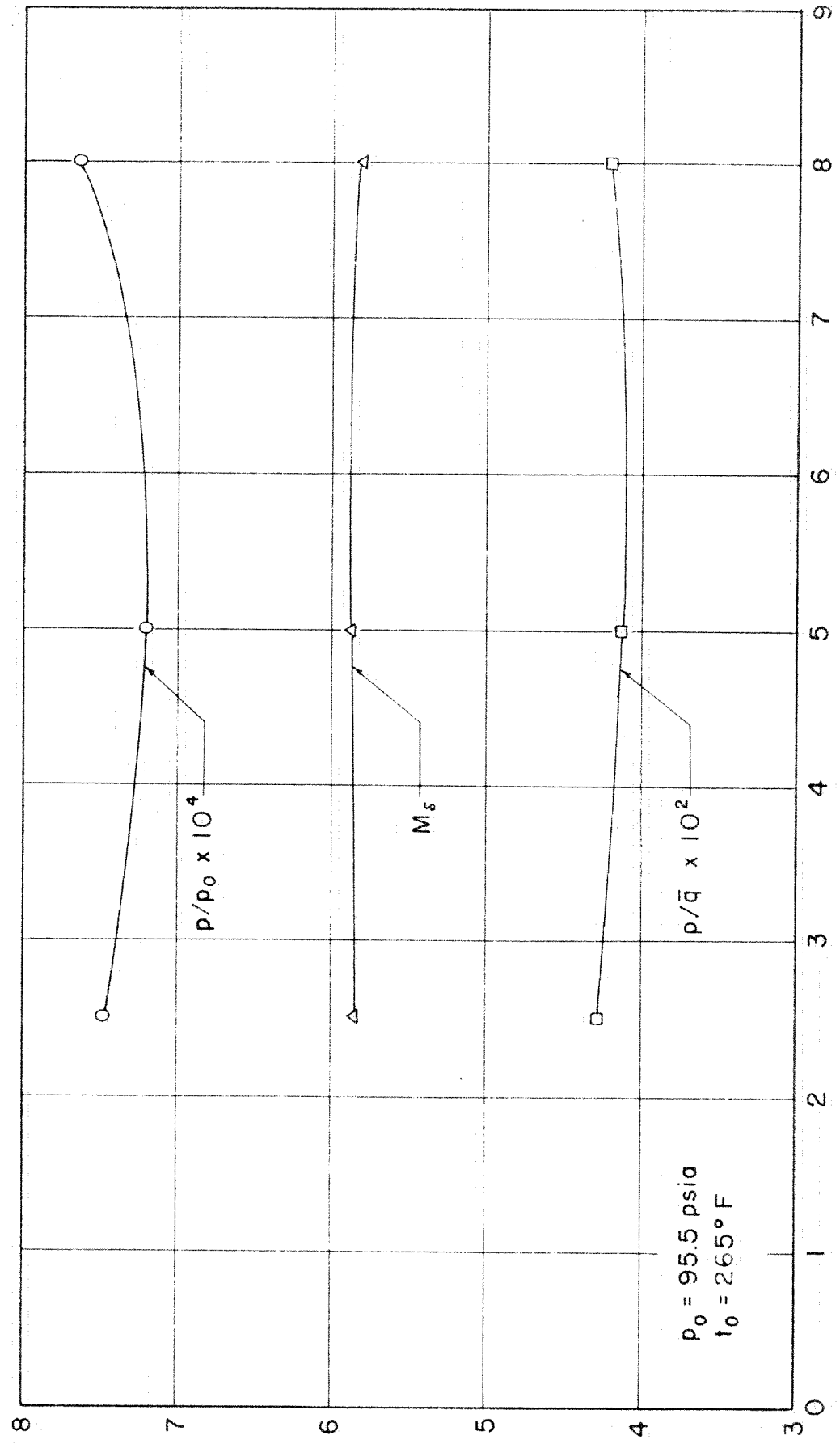

FIG. 12 REPRESENTATIVE p/p_o, MACH NUMBER AND $p/\bar{q}$ DISTRIBUTION ALONG THE PLATE

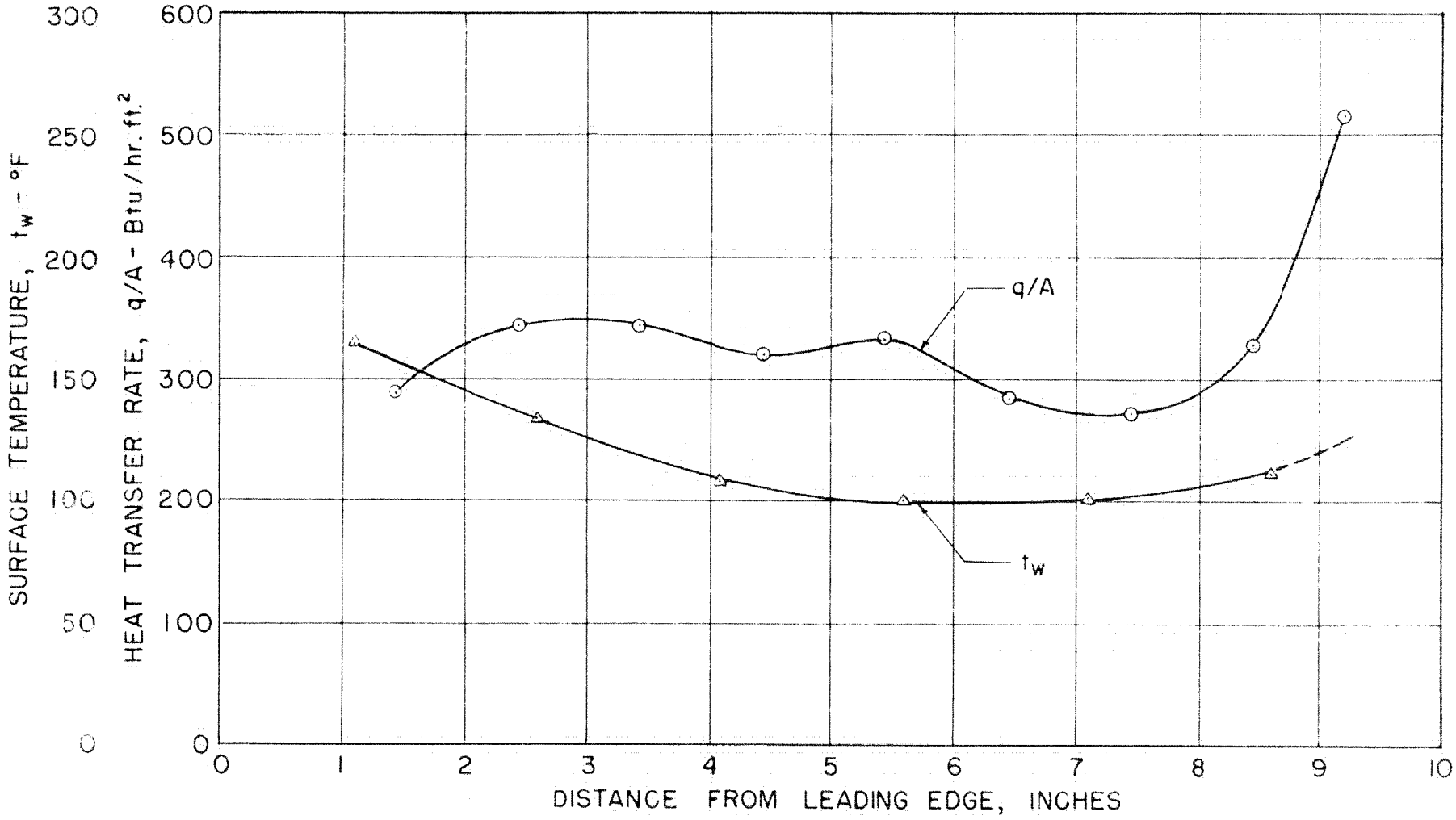

(a) STAGNATION PRESSURE, 115.5 psia
STAGNATION TEMPERATURE, 285°F

FIG. 13 REPRESENTATIVE CENTERLINE HEAT TRANSFER RATES AND SURFACE TEMPERATURES

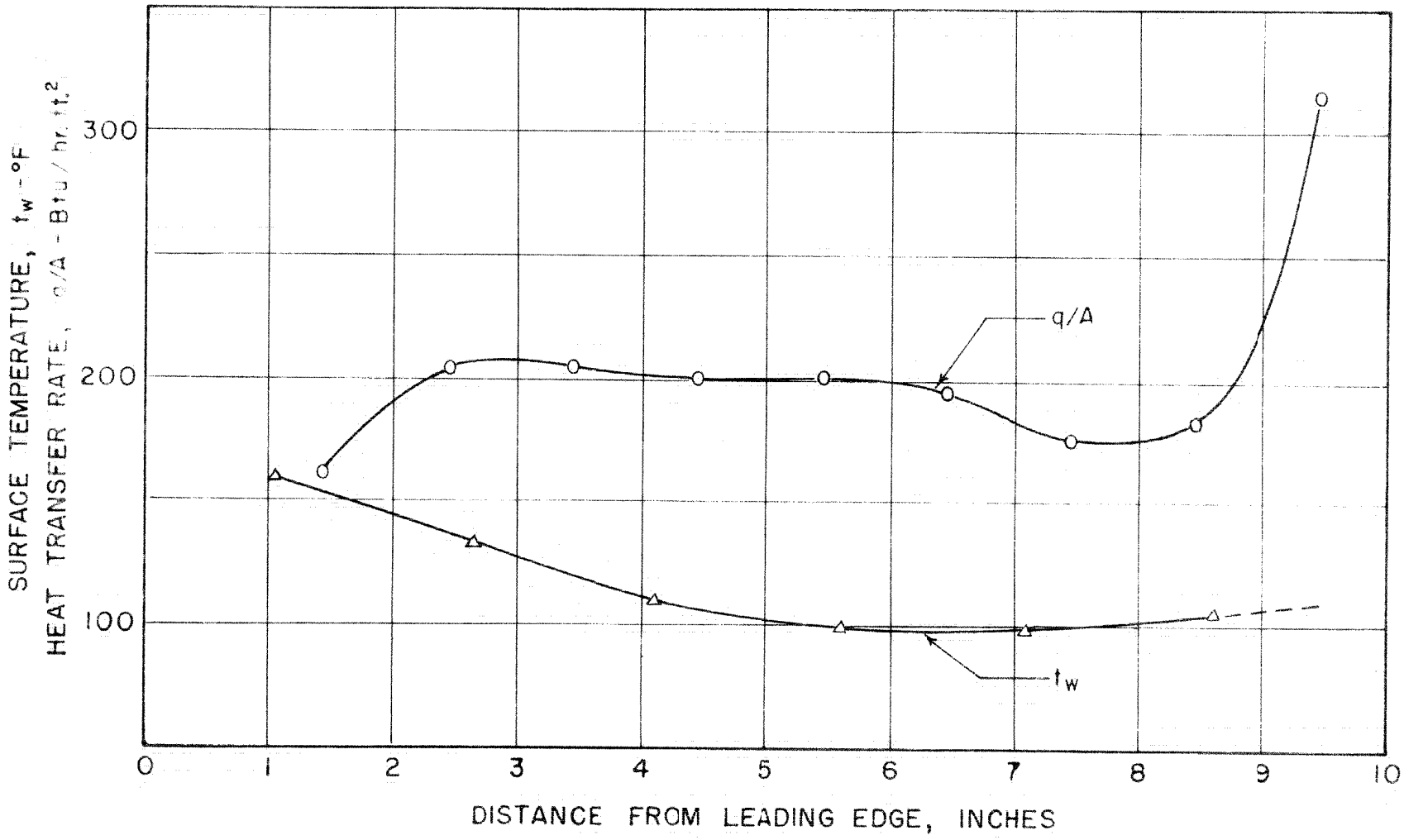

(b) STAGNATION PRESSURE, 95.5 psia
STAGNATION TEMPERATURE, 285°F

FIG. 13 CONTINUED

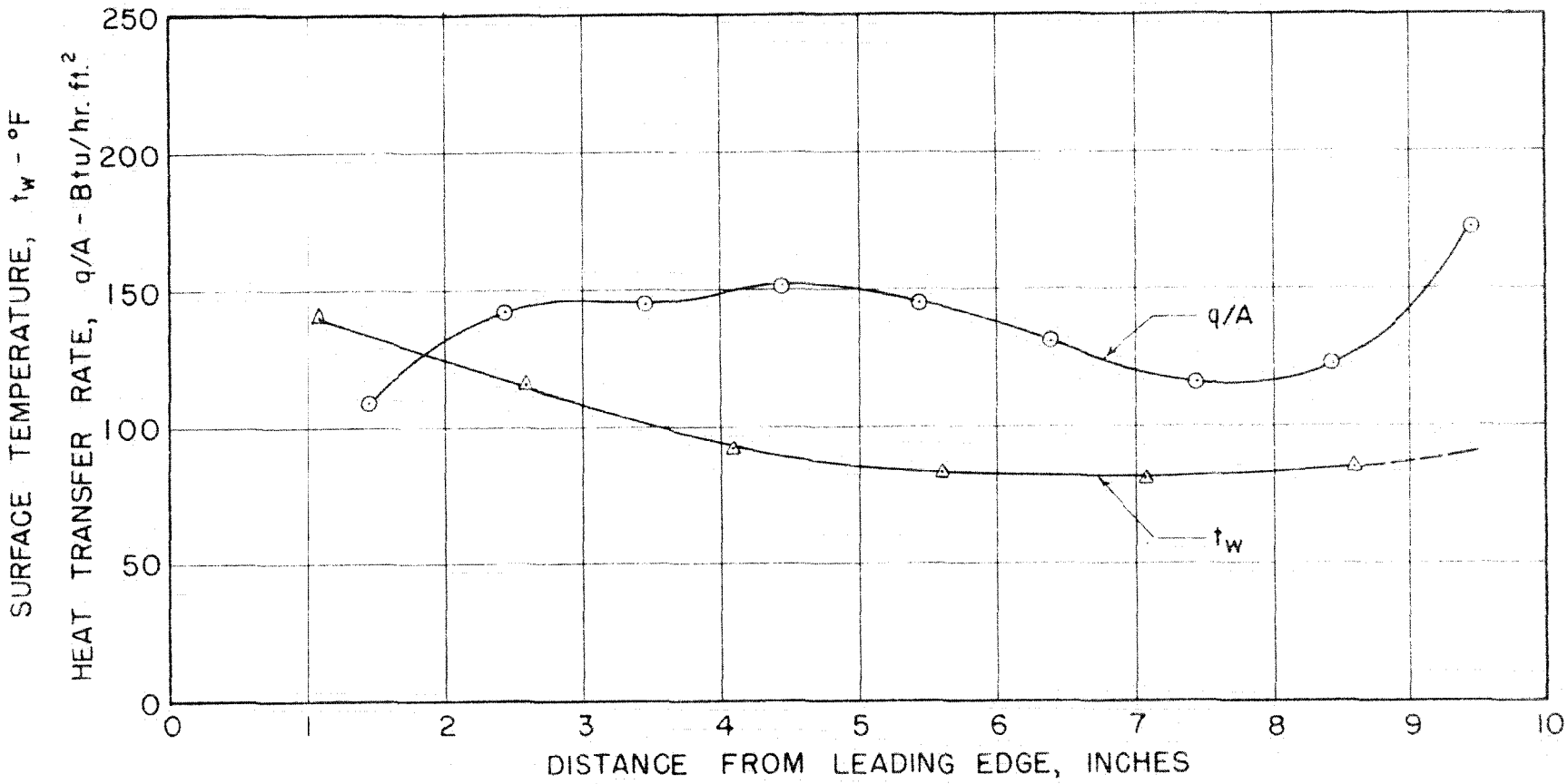

(c) STAGNATION PRESSURE, 75.5 psia
STAGNATION TEMPERATURE, 245°F

FIG. 13 CONTINUED

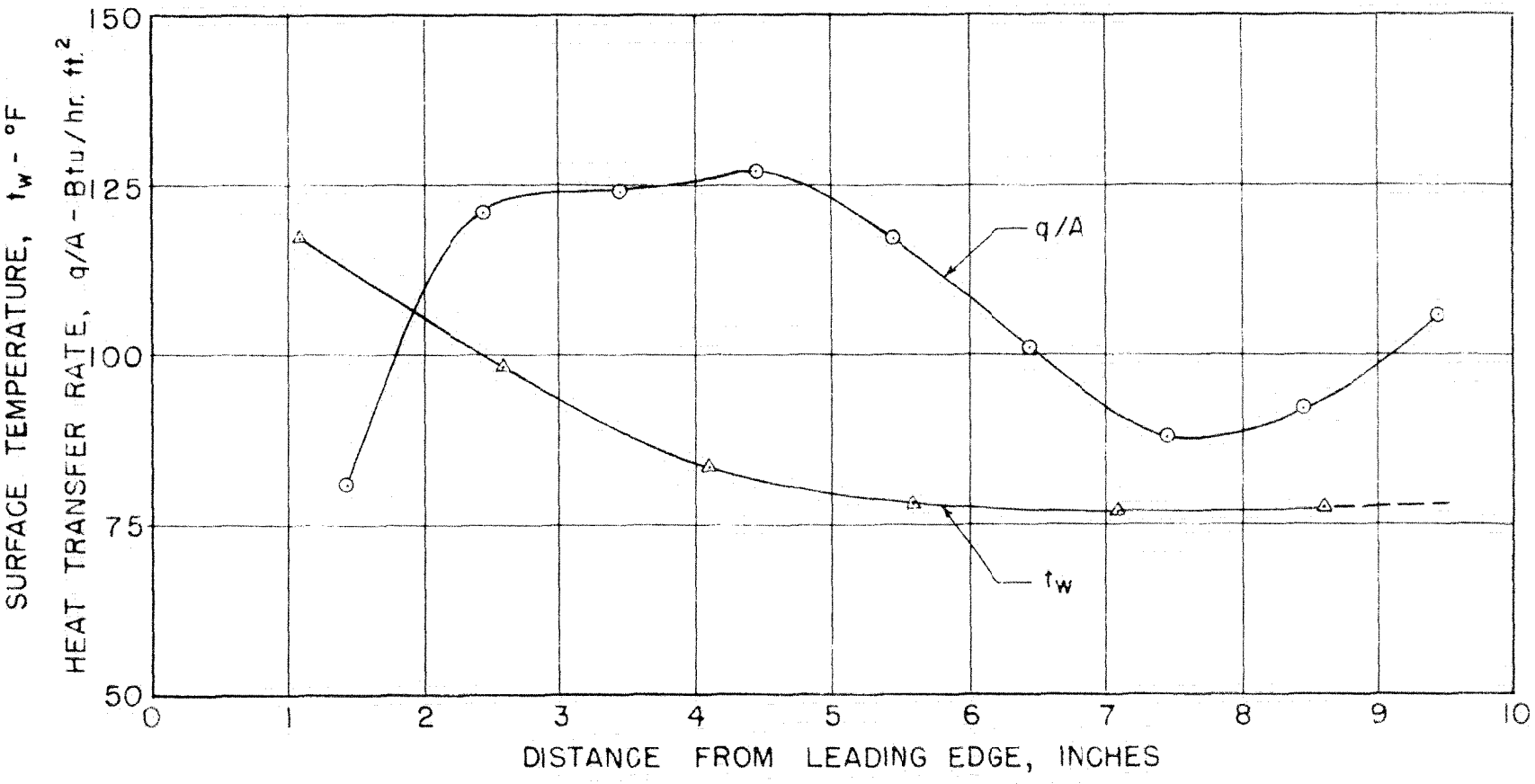

(d) STAGNATION PRESSURE, 60.4 psia
STAGNATION TEMPERATURE, 225°F

FIG. 13 CONCLUDED

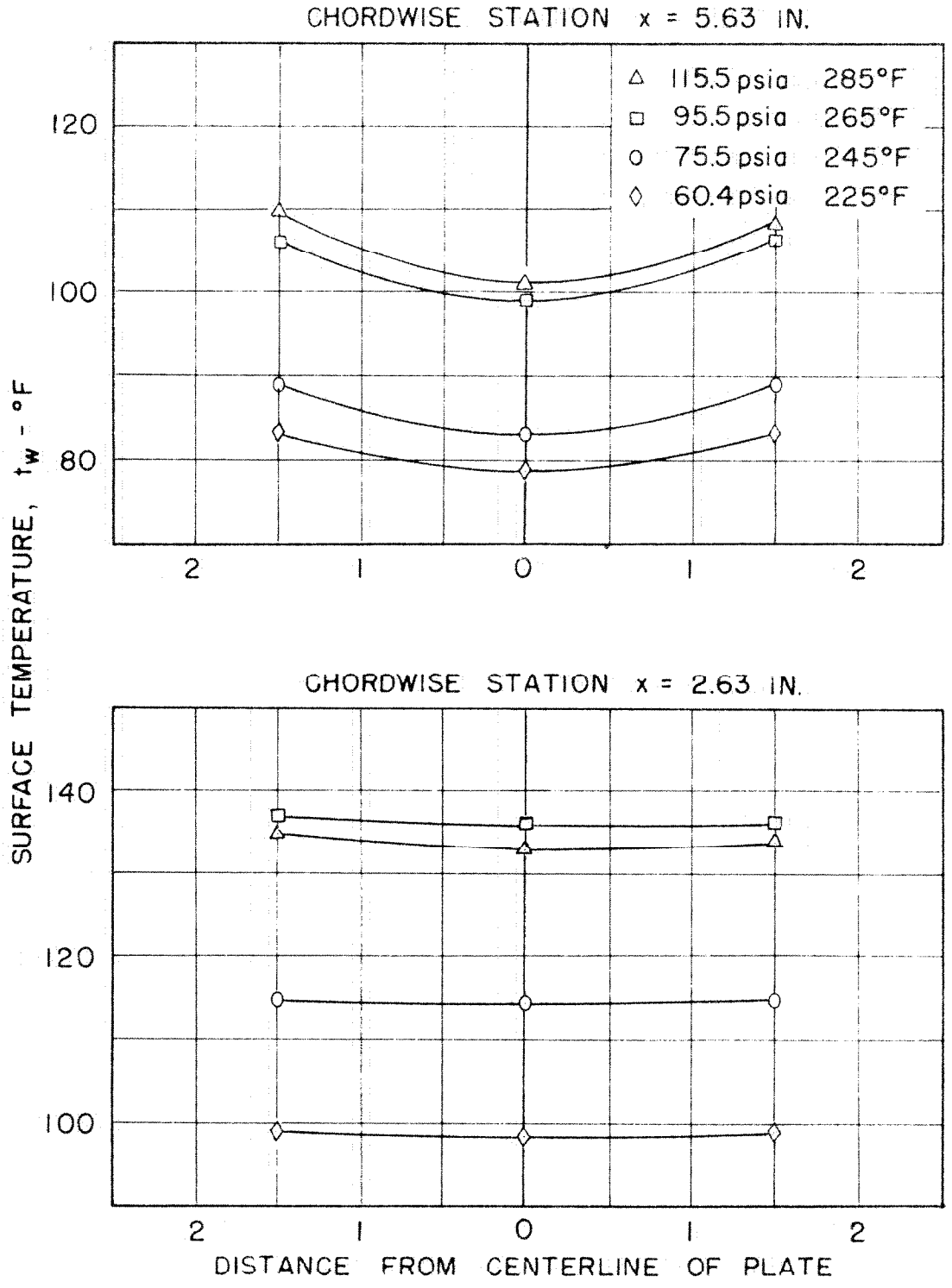

FIG. 14 REPRESENTATIVE SPANWISE TEMPERATURE DISTRIBUTION

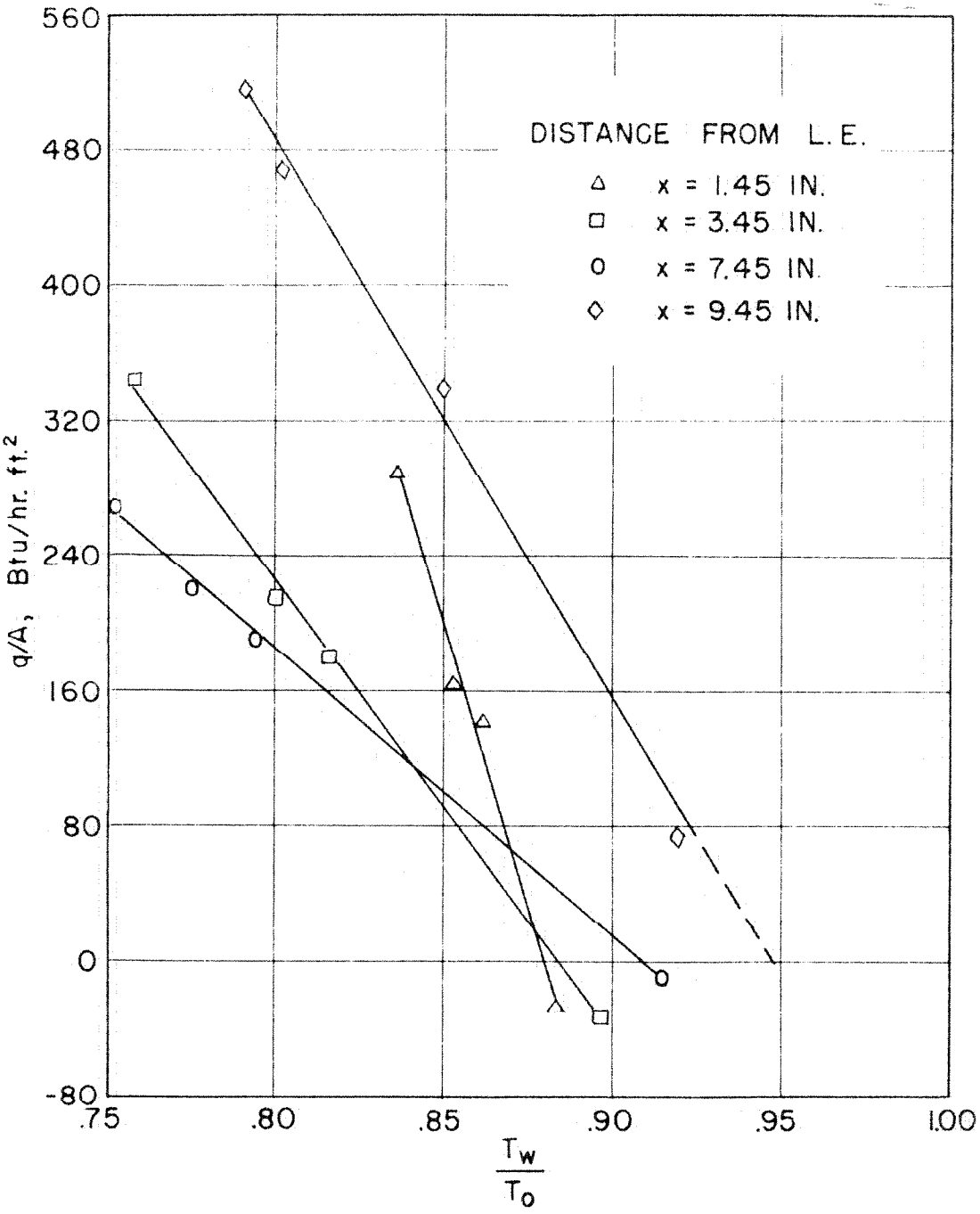

(a) STAGNATION PRESSURE, 115.5 psia

FIG. 15 VARIATION OF HEAT TRANSFER RATES WITH THE RATIO OF SURFACE TEMPERATURE TO STAGNATION TEMPERATURE

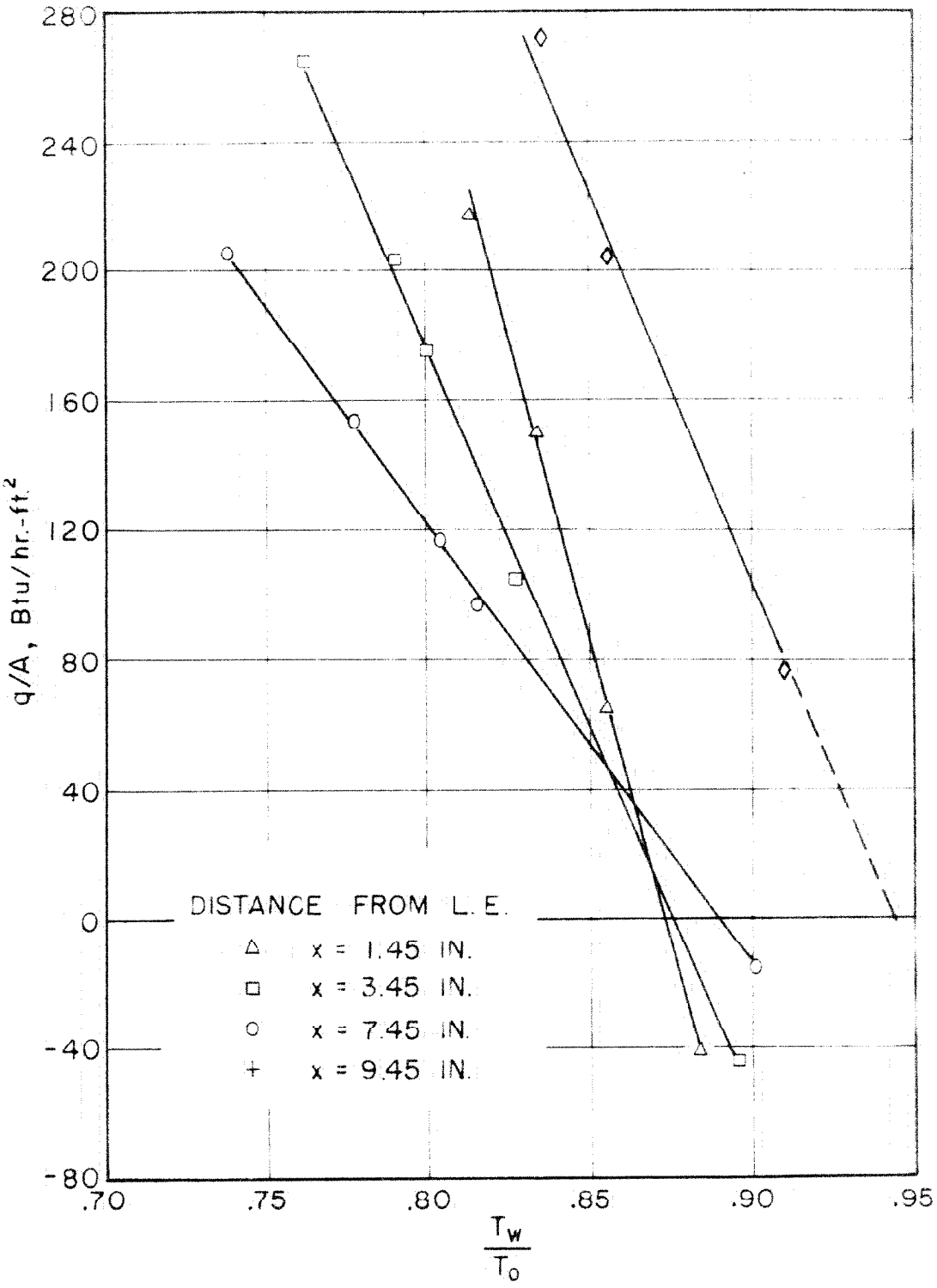

(b) STAGNATION PRESSURE, 95.5 psia

FIG. 15 CONTINUED

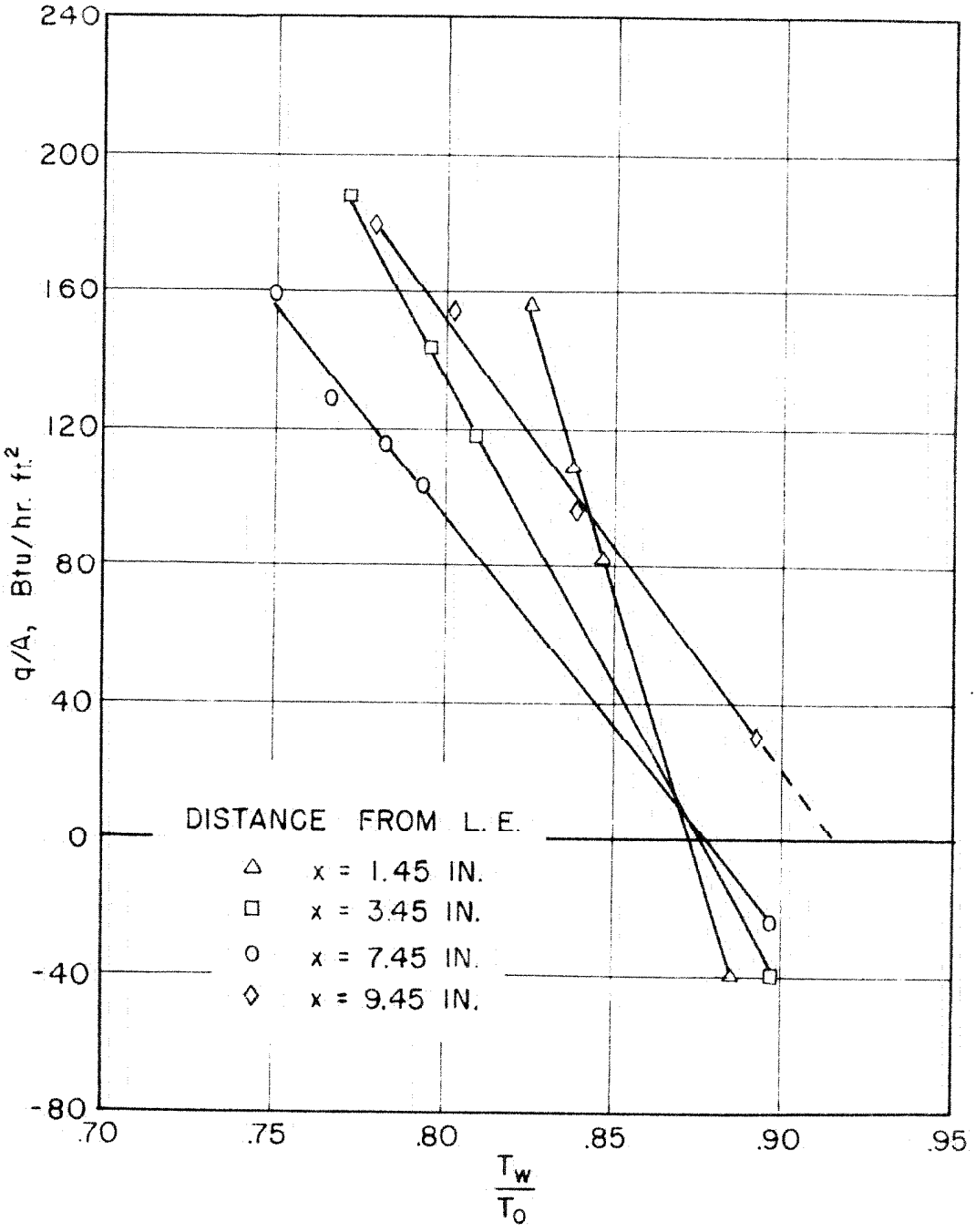

(c) STAGNATION PRESSURE, 75.5 psia

FIG. 15 CONTINUED

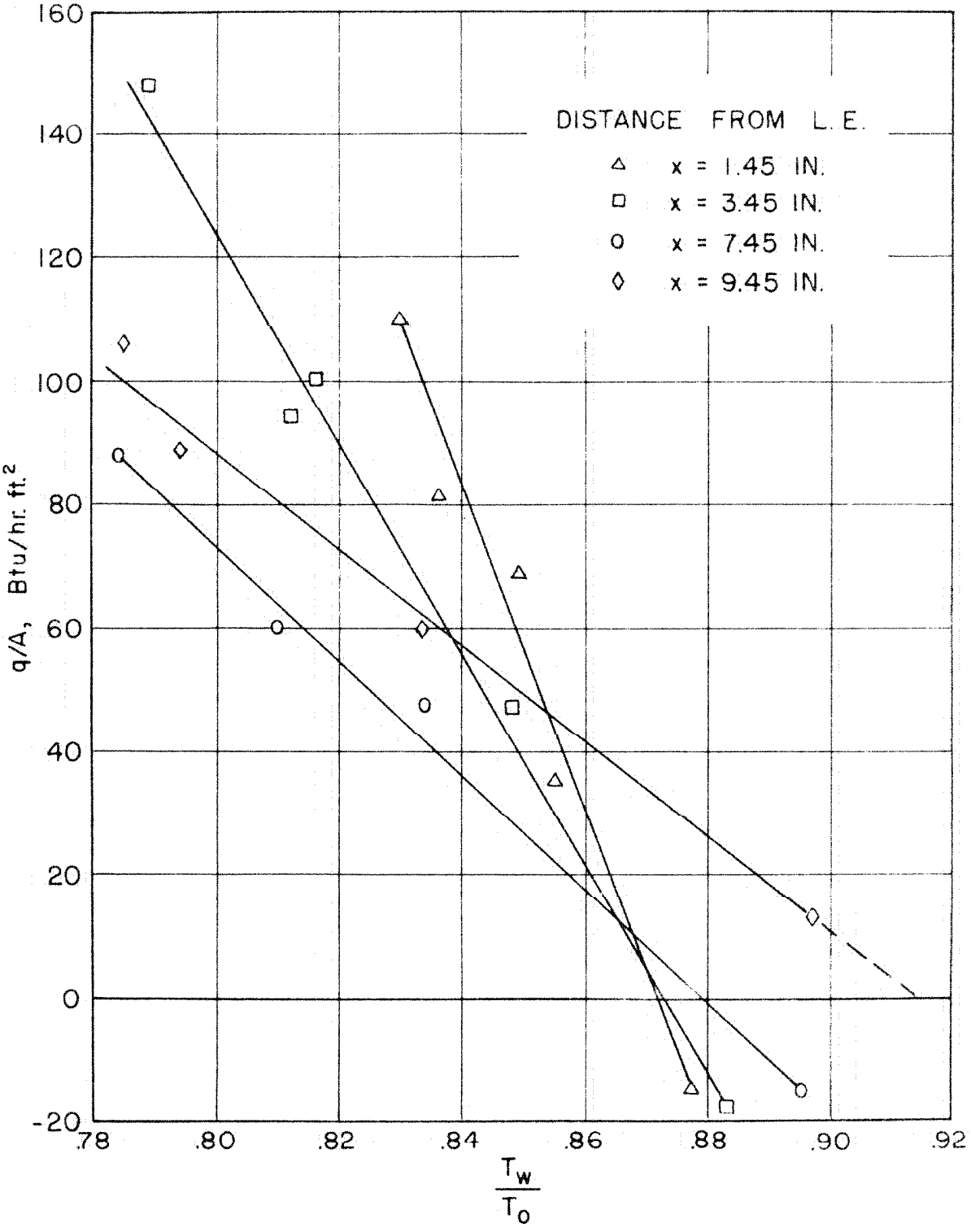

(d) STAGNATION PRESSURE, 60.4 psia

FIG. 15 CONCLUDED

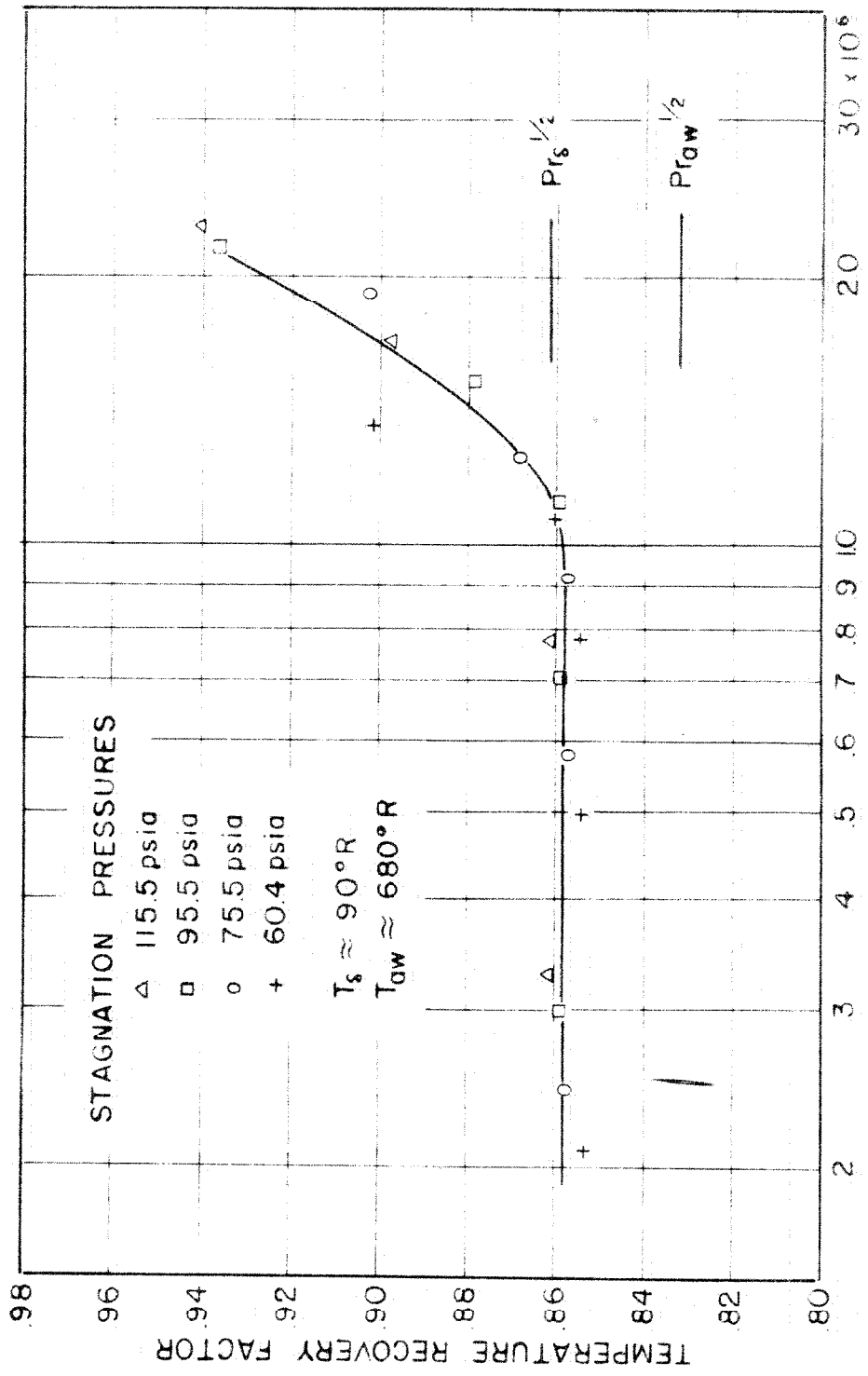

FIG. 16 EXPERIMENTAL TEMPERATURE RECOVERY FACTORS

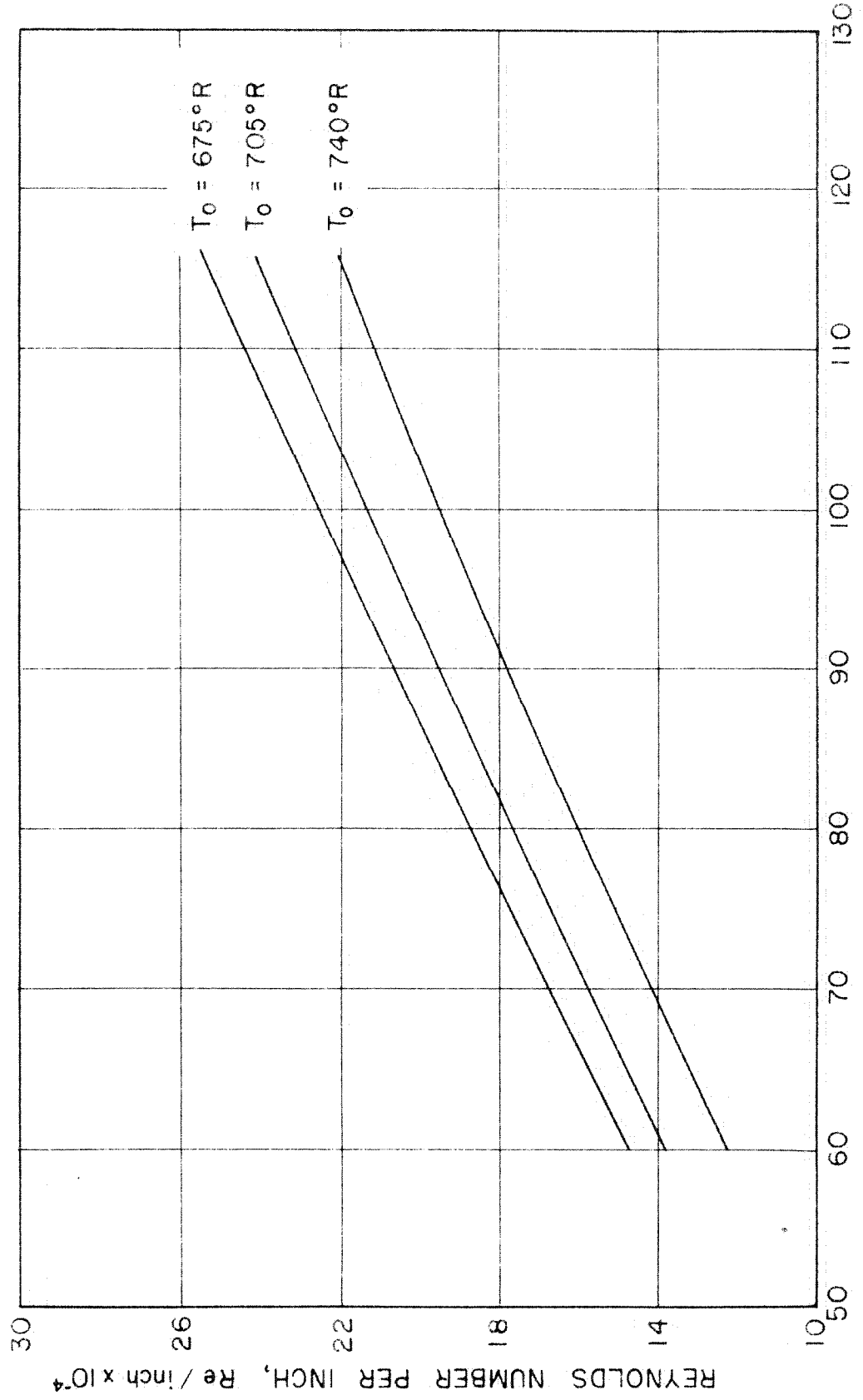

FIG. 17 FREE STREAM REYNOLDS NUMBER,

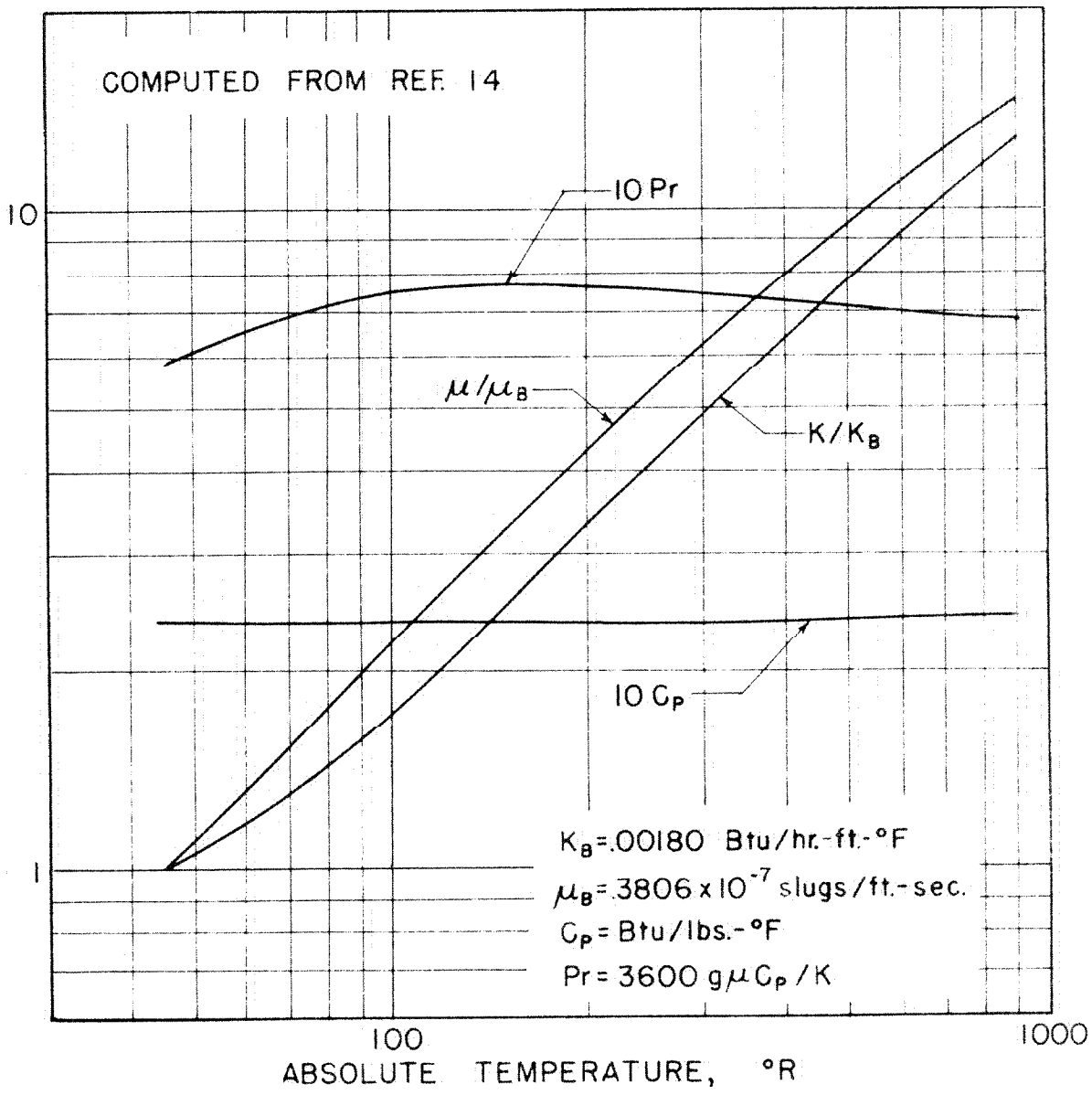

FIG. 18 AIR PROPERTIES

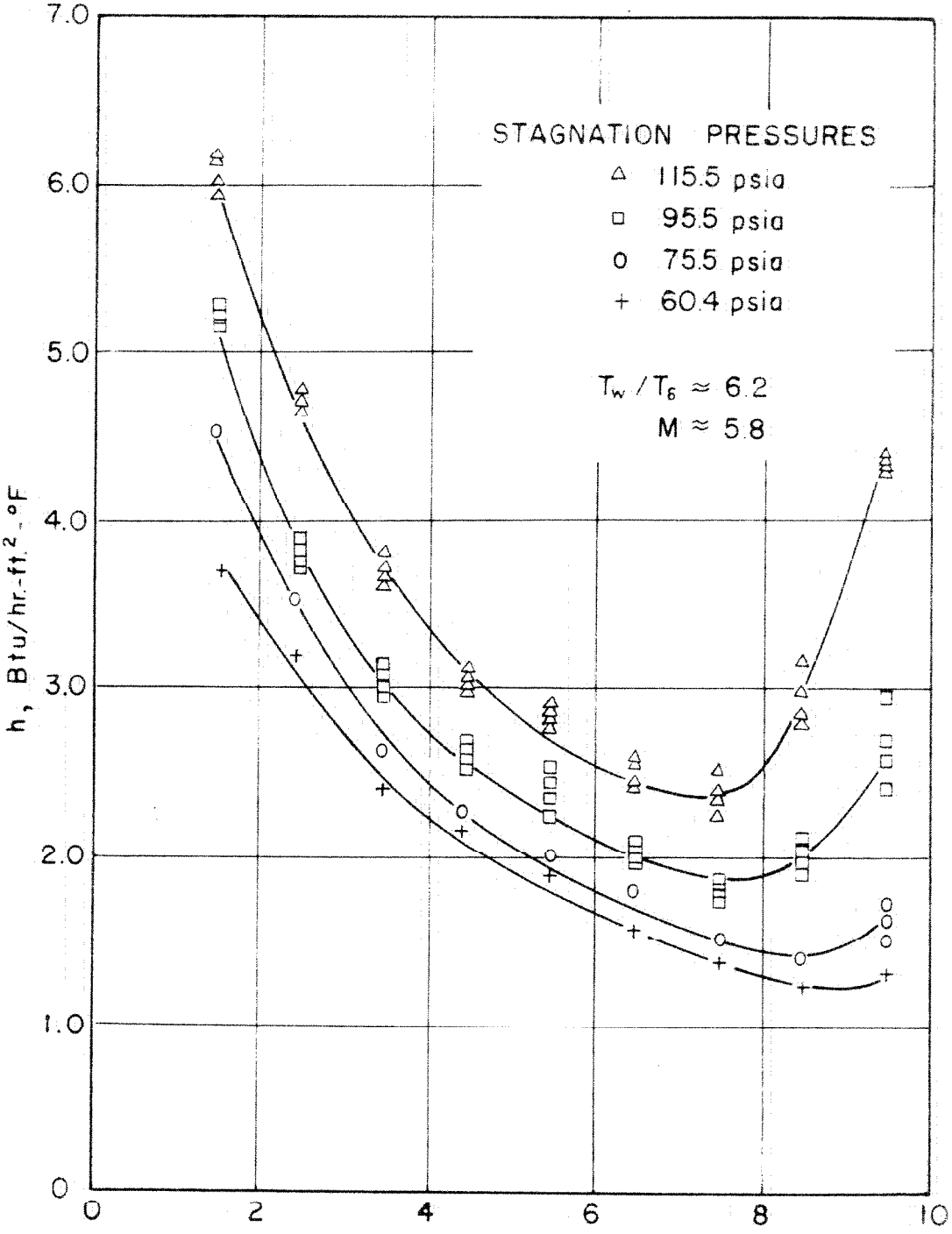

FIG. 19 EXPERIMENTAL HEAT TRANSER COEFFICIENTS

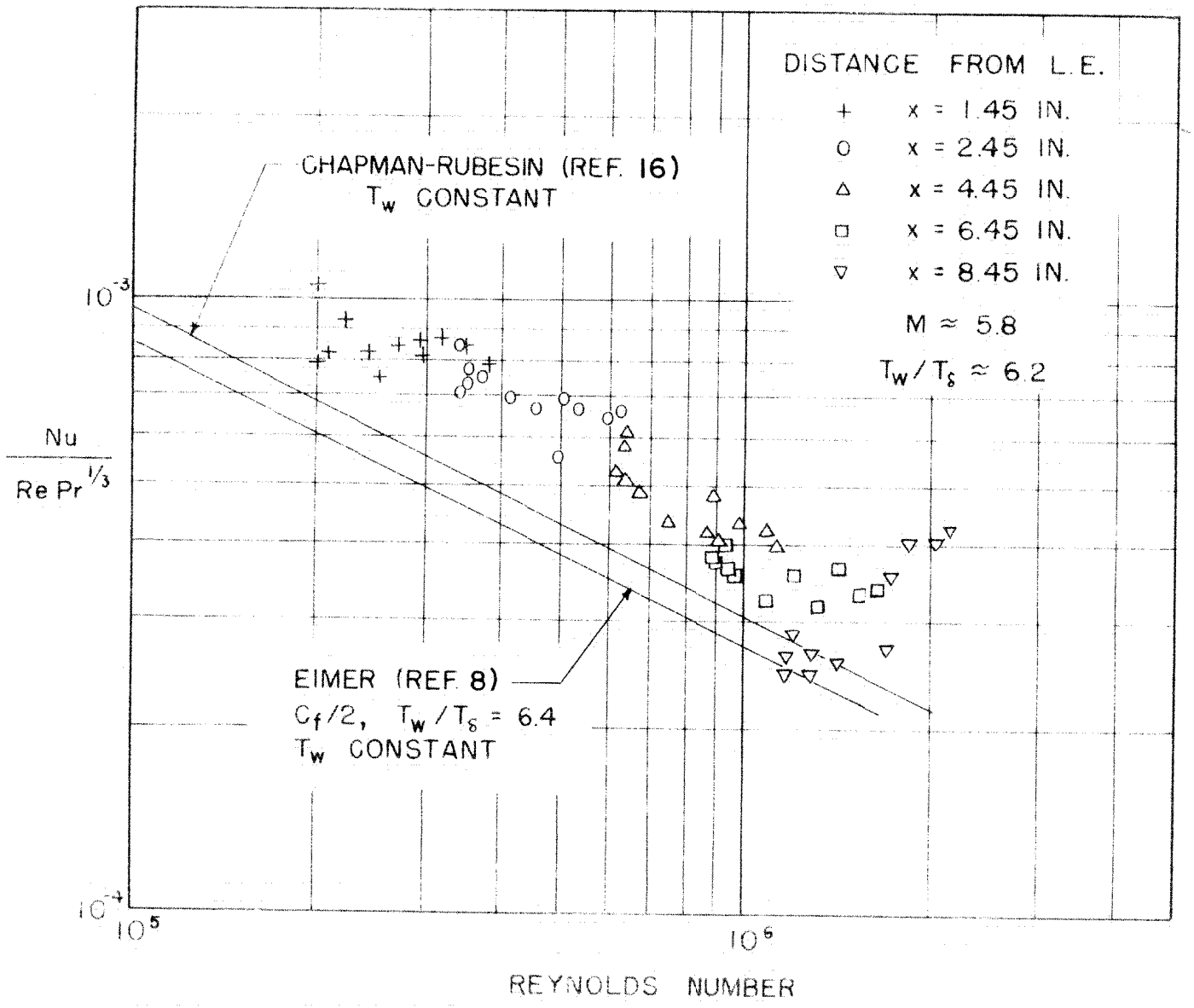

FIG. 20 DIMENSIONLESS REPRESENTATION OF HEAT TRANSFER DATA

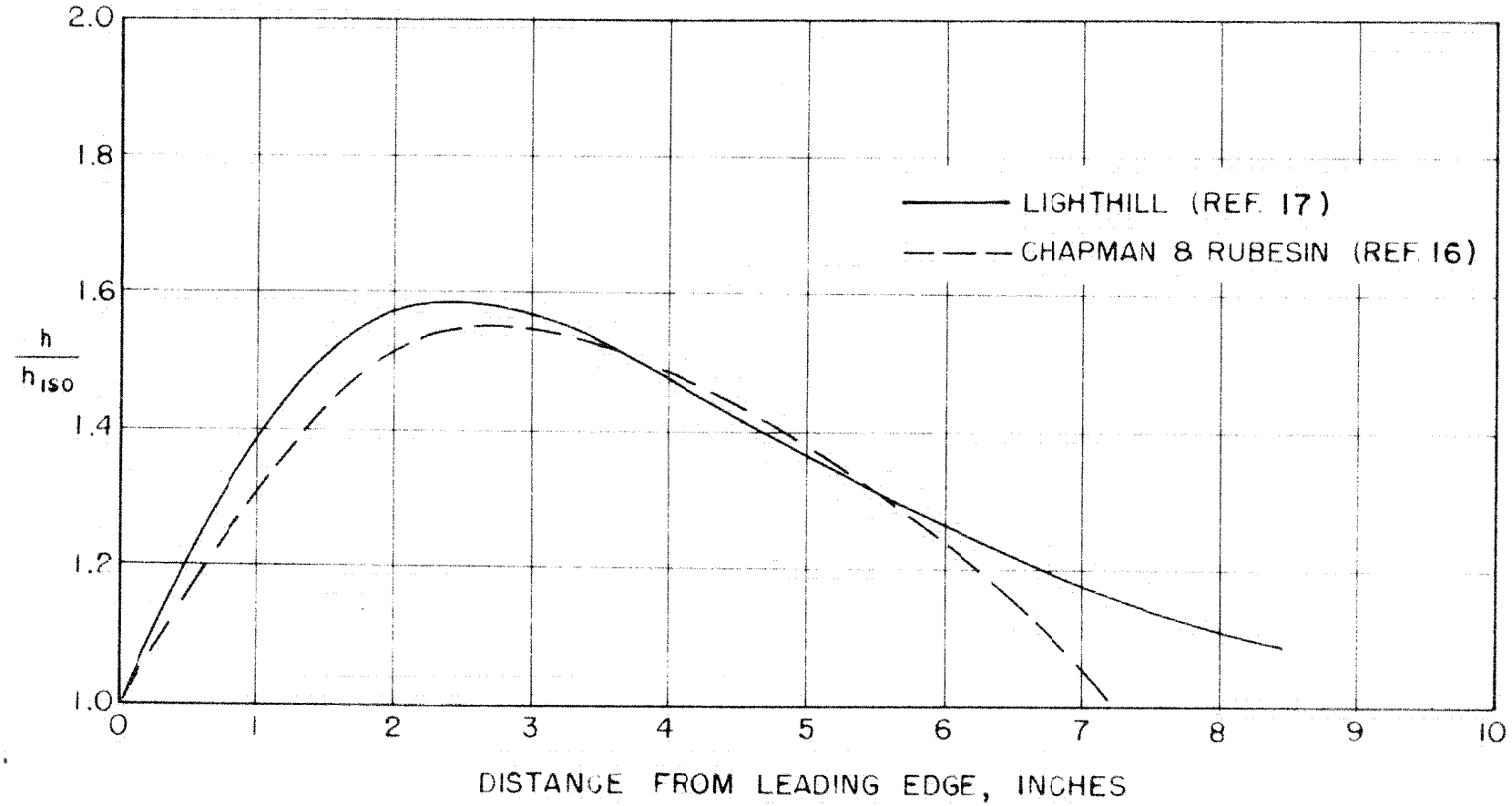

FIG. 21 REPRESENTATIVE RATIO OF EXPERIMENTAL HEAT TRANSFER COEFFICIENT TO ISOTHERMAL HEAT TRANSFER COEFFICIENT

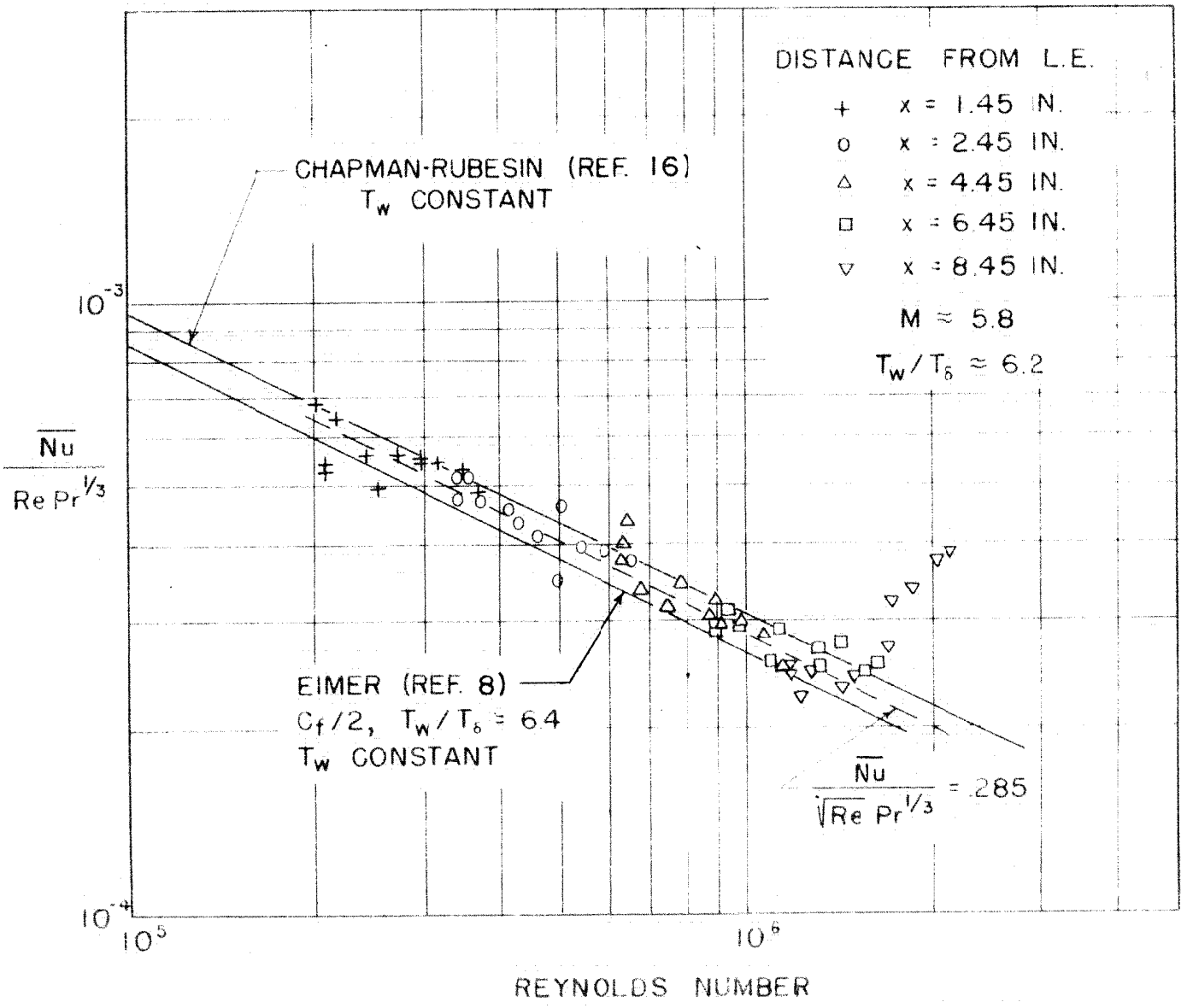

FIG. 22 DIMENSIONLESS REPRESENTATION OF HEAT TRANSFER DATA REFERRED TO THE CASE OF CONSTANT SURFACE TEMPERATURE

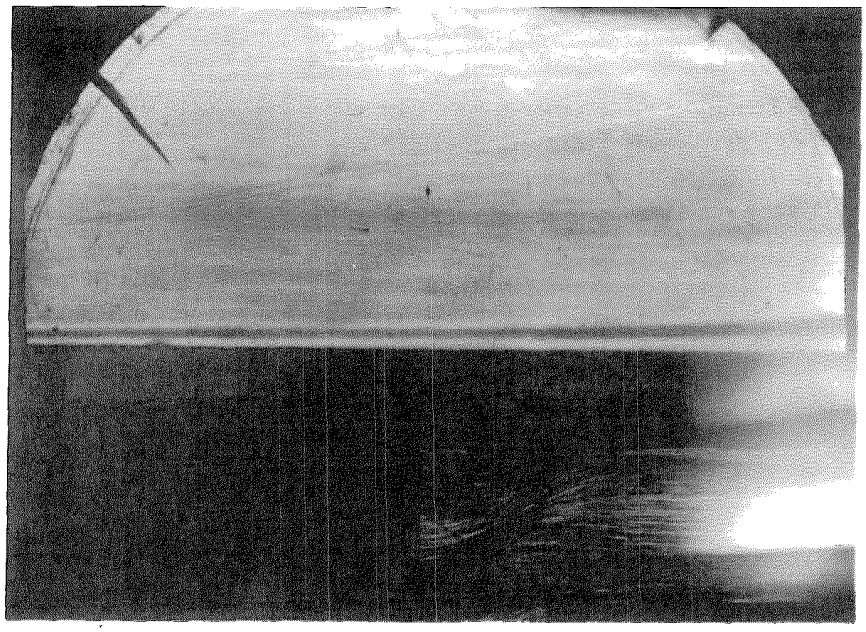

(a)

Before Separation

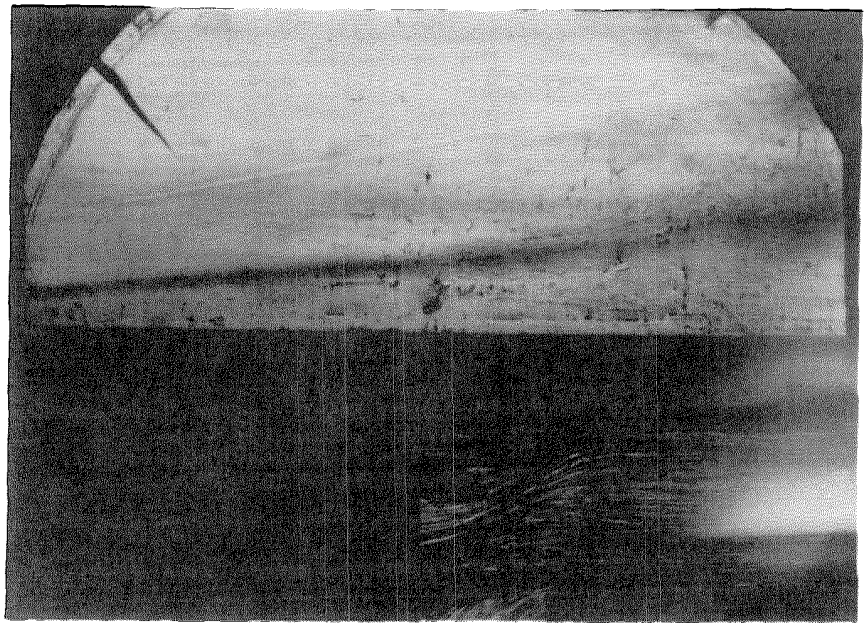

(b)

After Separation

Fig. 23

Separation of Laminar Boundary Layer

Re = 135,000/inch M = 5.7